Microbiological Research 289 (2024) 127922

Contents lists available at ScienceDirect

Microbiological Research

journal homepage: www.elsevier.com/locate/micres

Sterol regulatory element-binding proteins mediate intrinsic fungicide tolerance and antagonism in the fungal biocontrol agent *Clonostachys rosea* IK726

Edoardo Piombo [1], Georgios Tzelepis [1], Alma Gustavsson Ruus, Vahideh Rafiei, Dan Funck Jensen, Magnus Karlsson, Mukesh Dubey [*]

Department of Forest Mycology and Plant Pathology, Swedish University of Agricultural Sciences, Uppsala, Sweden

ARTICLE INFO

Keywords:
Ergosterol
Hypoxia tolerance
Iron homeostasis
Integrated pest management strategies
Lipid metabolism
SREBP
Sterol biosynthesis

ABSTRACT

Sterol regulatory element-binding proteins (SREBPs) are transcription factors governing various biological processes in fungi, including virulence and fungicide tolerance, by regulating ergosterol biosynthesis and homeostasis. While studied in model fungal species, their role in fungal species used for biocontrol remains elusive. This study delves into the biological and regulatory function of SREBPs in the fungal biocontrol agent (BCA) *Clonostachys rosea* IK726, with a specific focus on fungicide tolerance and antagonism. *Clonostachys rosea* genome contains two SREBP coding genes (*sre1* and *sre2*) with distinct characteristics. Deletion of *sre1* resulted in mutant strains with pleiotropic phenotypes, including reduced *C. rosea* growth on medium supplemented with prothioconazole and boscalid fungicides, hypoxia mimicking agent $CoCl_2$ and cell wall stressor SDS, and altered antagonistic abilities against *Botrytis cinerea* and *Rhizoctonia solani*. However, Δ*sre2* strains showed no significant effect. Consistent with the gene deletion results, overexpression of *sre1* in *Saccharomyces cerevisiae* enhanced tolerance to prothioconazole. The functional differentiation between SRE1 and SRE2 was elucidated by the yeast-two-hybridization assay, which showed an interaction between SREBP cleavage-activating protein (SCAP) and SRE1 but not between SRE2 and SCAP. Transcriptome analysis of the Δ*sre1* strain unveiled SRE1-mediated expression regulation of genes involved in lipid metabolism, respiration, and xenobiotic tolerance. Notably, genes coding for antimicrobial compounds chitinases and polyketide synthases were downregulated, aligning with the altered antagonism phenotype. This study uncovers the role of SREBPs in fungal BCAs, providing insights for *C. rosea* IK726 application into integrated pest management strategies.

1. Introduction

Integrated Pest Management (IPM) is a holistic and sustainable approach to pest management that aims to minimize the use of chemical pesticides, thereby diminishing risks to human health and the environment (Deguine et al., 2021). Biological control, which is defined as the use of living organisms (biological control agents, BCAs) for controlling insect pests, weeds and plant diseases, is one of the essential components of IPM and is considered crucial to reducing the use of pesticides in future agriculture production systems (Stenberg et al., 2021). Due to the inherent ability of certain BCAs to tolerate a relatively higher dose of specific fungicides compared with doses suggested for controlling fungal plant pathogens (Chaparro et al., 2011; Dubey et al., 2016, 2014a; Jensen et al., 2011; Tzelepis and Lagopodi, 2011; Wedajo, 2015), they can be combined with a low or full dose of compatible pesticides either simultaneously or in rotation, resulting in an enhanced degree of disease suppression of crop plants (Ons et al., 2020; Thambugala et al., 2020). Although the combined application of BCA with fungicides is considered a promising approach for future IPM strategies, a comprehensive knowledge of the BCAs' inherent ability to tolerate fungicides and their underlying mechanisms will help optimize the efficacy of BCA-fungicide combinations, which is of utmost importance for large-scale application under field conditions.

Ergosterol is an integral part of the fungal cell membrane and crucial for fungal survival; thus, enzymatic steps of ergosterol biosynthesis are widely used as a fungicide target for controlling fungal infections in crop

* Corresponding author.
E-mail address: Mukesh.dubey@slu.se (M. Dubey).
[1] Co-first author

https://doi.org/10.1016/j.micres.2024.127922
Received 1 July 2024; Received in revised form 10 September 2024; Accepted 25 September 2024
Available online 28 September 2024

plants (Yin et al., 2023). The ergosterol biosynthesis involves multiple enzymatic reactions and is regulated by the sterol regulatory element-binding protein (SREBP) family of transcription factors. In the fission yeast *Schizosaccharomyces pombe* and in the human pathogens *Cryptococcus neoformans* and *Aspergillus fumigatus*, for example, at optimum ergosterol concentration, SREBP is bound to the SCAP (SREBP cleavage activating protein), and the complex is retained at the endoplasmic reticulum (ER) by associating with Insulin-induced gene (INSIG) (Espenshade and Hughes, 2007). SCAP dissociates from INSIG at low ergosterol levels, releasing the SREBP-SCAP complex. The complex is then further transported to the Golgi apparatus, where the N-terminus of the SREBP is released from SCAP by proteolytic cleavage by two proteases (Espenshade and Hughes, 2007). The release enables SREBP to travel to the nucleus to induce the expression of genes involved in lipid biosynthesis and uptake (Espenshade and Hughes, 2007). The regulatory role of SREBPs is carried out by a basic helix loop helix (bHLH) leucine zipper DNA binding domain with a unique tyrosine residue at the N-terminus (Bien and Espenshade, 2010), while interaction between SREBP and SCAP is mediated by a domain of unknown function (DUF2014) (Maguire et al., 2014). By regulating ergosterolhomeostasis and uptake, SREBPs mediate several biological processes in fungi, including carbohydrate metabolism, fungicide tolerance, hypoxia adaptation, and iron homeostasis (Espenshade and Hughes, 2007). The role of SREBPs in fungal virulence is also demonstrated in human pathogenic fungi such as *C. neoformans* and *A. fumigatus*, and plant pathogenic fungi such as *Pyricularia oryzae* (previously *Magnaporthe oryzae*) and *Penicillium digitatum* (Chung et al., 2019; Osborne and Espenshade, 2009; Ruan et al., 2017). The evidence includes functional analysis by generating SREBP gene deletion strains and comparing their virulence phenotype to the wild type (Chung et al., 2019; Osborne and Espenshade, 2009; Ruan et al., 2017). However, while the role of SREBPs in all these processes has been shown in yeast and filamentous fungal species pathogenic to humans and plants, their role in fungal species used for biocontrol of fungal diseases remains elusive. This study aimed to investigate the biological and regulatory functions of SREBPs in fungal BCAs, focusing on their roles in xenobiotic (fungicide) tolerance and antagonism, which are hallmarks of fungi used as BCAs.

To achieve this aim, we used *Clonostachys rosea* strain IK726 (phylum Ascomycota, order Hypocreales)- a soil-borne filamentous fungus commonly known for its biocontrol capability against various plant-pathogenic fungi (Funck Jensen et al., 2021; Sun et al., 2020). Competition for nutrients and space, mycoparasitism, and interference competition through antibiosis are important biocontrol traits of *C. rosea* (Funck Jensen et al., 2021; Sun et al., 2020). Moreover, the tolerance of *C. rosea* to toxic fungal compounds has also been shown to contribute to its biocontrol ability (Dubey et al., 2016, 2014a; Kosawang et al., 2014). In addition, *C. rosea* has shown tolerance to chemical fungicides of various modes of action (Dubey et al., 2014a; Jensen et al., 2011; Macedo et al., 2012; Roberti et al., 2006; Tzelepis and Lagopodi, 2011), making it a promising candidate for IPM strategy.

The development of fungicide tolerance may evolve through various mechanisms, including alterations in cellular processes involved in fungicide uptake, target site modification and enforcement, metabolic detoxification and epigenetic changes altering gene expression (Yin et al., 2023). We hypothesized that SREBPs contribute to intrinsic fungicide tolerance and interspecies fungal interactions by regulating ergosterol metabolism and xenobiotic efflux. Our results show that *C. rosea* contains genes required for SREBP-mediated ergosterol homeostasis. By generating gene deletion and complementation strains, we demonstrate the role of SREBPs in fungicide tolerance and antagonisms in *C. rosea*. Furthermore, through comparative transcriptome analysis of the SREBP deletion strains and *C. rosea* wild type (WT), we elucidated the SREBP-mediated transcriptional reprogramming of genes associated with lipid and carbohydrate metabolism, xenobiotic tolerance, and antagonism.

2. Material and methods

2.1. Fungal strains and culture conditions

Clonostachys rosea strain IK726 WT and mutants derived from it, *B. cinerea* strain B05.10, *Fusarium graminearum* strain PH-1, *R. solani* SA1 were maintained on potato dextrose agar (PDA; Oxoid, Cambridge, UK) medium at 20°C. The yeast strains were maintained on YPD medium (in g/L; yeast extract 10, peptone 20, dextrose 20) at 30 °C. Unless otherwise specified, the Czapek dox (CZ) medium (Sigma-Aldrich, St. Louis, MO) was used for phenotypic analyses.

2.2. Gene identification and sequence analysis

The *C. rosea* strain IK726 genome version 1 (Karlsson et al., 2015) and version 2 (Broberg et al., 2018) were screened for genes encoding SREBP, INSIG, and SCAP using BLASTP analysis. The presence of conserved domains was analysed with the Simple modular architecture research tool (SMART) (Letunic et al., 2009), InterProScan (Jones et al., 2014) and conserved domain search (CDS) (Marchler-Bauer et al., 2011). The presence of Tyrosine residues in SREBPs in specific spacing patterns was analysed manually. TOPCONS (http://topcons.net/; Tsirigos et al., 2015) and TMHMM-2.0 were used to predict the transmembrane domain and signal peptide . Amino acid (aa) sequence alignment was performed using ClustalW2 (Larkin et al., 2007) with default settings for multiple sequence alignment.

2.3. Comparative genomics analysis

All the published proteomes of Hypocreales species were downloaded from Mycocosm (Ahrendt et al., 2022). The genera *Fusarium*, *Metarhizium*, *Ophiocordyceps*, *Stachybotrys*, *Tolypocladium* and *Trichoderma* had a high number of annotated species, and therefore, only three species per genus were considered (**Supplementary Table 1**). Each proteome was annotated with InterProScan v. 5.48–83.0 (with options "–iprlookup –goterms –pathways") (Jones et al., 2014). Proteins showing both Pfam and InterProScan family "Insulin-induced protein" (PF07281 and IPR025929) were considered putative INSIG proteins. Proteins showing family "Sterol regulatory element-binding protein cleavage-activating" (IPR030225) and the sterol sensing domain (IPR000731) were considered putative SCAP proteins. Proteins having both domain bHLH (IPR011598) and domain "Sterol regulatory element-binding protein 1, C-terminal" (IPR019006) were considered to be putative SRE1 homologs. SRE2 proteins are short, and the only domain-based filtering in their prediction was the presence of the bHLH domain, resulting in a high number of candidates. For this reason, they were further filtered by excluding proteins with no blast matches on any of the SRE proteins predicted in the work of Chung et al. (2019). This last analysis was carried out with BLASTP v. 2.11.0 (with options "-e value 1e-10 -qcov_hsp_perc 80") (Altschul et al., 1990). All the proteins considered are listed in **Supplementary Table 1**.

2.4. Domain-wise phylogenetic analysis

INSIG and SCAP proteins were identified as described previously in the species considered in the work by Chung et al. (2019), namely *A. fumigatus* (GCF_000002655.1), *A. nidulans* (GCF_000011425.1), *Candida albicans* (GCF_000182965.3), *C. graminicola* (GCF_000149035.1), *F. graminearum* (GCF_000240135.3), *F. oxysporum* (GCF_000271745.1), *P. oryzae* (GCF_000002495.2), *Neurospora crassa* (GCF_000182925.2), *S. cerevisiae* (NM_001184673.1) and *S. pombe* (NM_001018252.2). SRE proteins in these species were not identified through a new analysis, but the same proteins utilized in Chung et al. (2019) were considered.

One phylogenetic tree was obtained for each of the INSIG, SCAP and SREBP classes, considering only the domain PF07281 in INSIG proteins,

domain IPR000731 in SCAP proteins and domain IPR011598 in SREBPs. Domain locations were predicted with InterProScan v. 5.48–83.0 (Jones et al., 2014), extracted with SAMtools v. 1.11 (Danecek et al., 2021) and aligned with MAFFT v. 7.453 (with options "–max iterate 1000 –localpair") (Katoh and Standley, 2013). The trees were obtained with IQ-TREE v. 2.1.3 (with options "-m MFP -b 1000 -T 1 -safe") (Minh et al., 2020). The best-fit models chosen by the ModelFinder function of IQ-TREE were Q.plant+G4 for INSIG proteins, mtZOA+G4 for SCAP proteins and JTT+G4 for SRE proteins. After 1000 bootstraps, the SRE tree nodes with bootstrap values less than 50 % were condensed through MEGA v. 10.0.5 to improve readability (Kumar et al., 2018). and the tree figures were improved with Scientific Inkscape (https://github.com/burghoff/Scientific-Inkscape/tree/main).

2.5. Yeast-two-hybrid assays

For the yeast-two-hybrid (Y2H) assay, *sre1*, *sre2*, and *scap* genes were amplified from *C. rosea* cDNA using gene-specific primers (**Supplementary Table 2)** and subcloned to the pDONOR/Zeo donor vector (Thermo Fisher, MA). The donor vectors were cloned either to the pGADT7-GW prey or the pGBKT7-GW bait plasmids using Matchmaker Gold Yeast Two-Hybrid System (Takara, Kusatsu, Japan) and simultaneously transformed to the *S. cerevisiae* AH109 strain following manufacturer protocol (Takara, Kusatsu, Japan). Transformation with empty vectors was used as a negative control. Positive colonies were selected on Synthetic minimal (SD) -Leu, -Trp, media and potential protein interactions were evaluated on SD -His, -Ade, -Leu, -Trp media. Five replicates per interaction have been used.

2.6. Heterologous expression of sre1 and sre2 in Saccharomyces cerevisiae

For heterologous expression in *S. cerevisiae*, the *sre1* and *sre2* genes were amplified using cDNA from *C. rosea* and cloned to the pYES-2 vector driven by *GAL1* promoter, using the GeneArt™ Seamless Cloning and Assembly Enzyme Mix (Thermo Fisher Scientific, MA) according to manufacturers' instructions. The vectors were transformed using a polyethene glycol-based protocol in the BY4742 strain (Agatep et al., 1998) and positive transformants were selected on Synthetic Complete (SC) -Ura media. Transformation with the empty pYES-2 vector was used as a negative control. For gene induction, overexpression strains were precultured in SC -Ura media with 2 % raffinose to reach the log phase. Then, the OD_{600} was adjusted to 0.3 and transferred to SC -Ura media supplemented with 2 % galactose. The growth of *S. cerevisiae* strains was investigated in SC -Ura medium supplemented with 1.5 ppm prothioconazole dissolved in 50 % DMSO (Merck, NJ) and measuring the OD_{600} in SpectraMax Gemini™ XPS/EM microplate reader (Molecular Devices, CA) at 30 °C in a time-course assay. In control treatment, prothioconazole was replaced with an equal volume of 50 % DMSO. The experiment was performed with six biological replicates. The optimum concentration of prothioconazole was selected by successive screening of the *S. cerevisiae* strain to a prothioconazole concentration ranging from 0.1 ppm to 5 ppm.

2.7. Construction of deletion vector, transformation, and mutant validation

The ~ 1 kb 5′-flank and 3′-flank regions of *sre1* and *sre2* were amplified from the genomic DNA of *C. rosea* using gene-specific primer pairs as indicated in **Supplementary Figure 1**. Gateway entry clones of the purified 5′-flank and 3′-flank PCR fragments were generated as described by the manufacturer (Invitrogen, Carlsbad, CA). The hygromycin resistance cassette (hygB) generated during our previous studies (Dubey et al., 2012) from the pCT74 vector, as well as a geneticin resistance cassette generated as a PCR product from the pUG6 vector (Güldener et al., 1996), were used. The gateway LR recombination reaction was performed using the entry plasmid of respective fragments and destination vector pPm43GW (Karimi et al., 2005) to generate the deletion vectors. A complementation cassette for *sre1* was constructed by amplifying the full-length sequence of *sre1,* including more than 1 kb upstream and around 500 bp downstream regions from the genomic DNA of *C. rosea* WT (**Supplementary Table 2; Supplementary Figure 1).** The amplified DNA fragments were purified and integrated into the destination vector pPm43GW using Gateway cloning technology (Invitrogen, CA) to generate complementation vectors.

Agrobacterium tumefaciens-mediated transformation (ATMT) was performed based on a previous protocol for *C. rosea* (Utermark and Karlovsky, 2008). Transformed strains were selected on plates containing hygromycin for gene deletion and geneticin for complementation. Validation of homologous integration of the deletion cassettes in putative transformants was performed using a PCR screening approach with primer combinations targeting the hygB cassette and sequences flanking the deletion cassettes **(Supplementary Figure 1**), as described previously (Dubey et al., 2013a, 2013b). The PCR-positive transformants were purified by two rounds of single spore isolation (Dubey et al., 2012). The transcript levels of *sre1* and *sre2* on WT, and respective gene deletion and complementation strains, were determined by reverse transcription polymerase chain reaction (RT-PCR) using RevertAid premium reverse transcriptase (Fermentas, St. Leon-Rot, Germany) and their respective primer pairs (**Supplementary Table 2; Supplementary Figure 1**).

Phenotypic analyses were performed with *C. rosea* WT, three independent single deletion strains of *sre1* (Δ*sre1_1*, Δ*sre1_5*, Δ*sre1_15*) and *sre2* (Δ*sre2_14*, Δ*sre2_55*, Δ*sre2_104*) and *sre1* complemented strain Δ*sre1*+. Each experiment included three to five biological replicates (depending on the phenotype), and each experiment was repeated two times with similar results unless otherwise specified.

2.8. Phenotypic analyses

For growth rate analysis, a 3 mm diameter agar plug from the growing mycelial front was transferred to solid CZ medium or CZ medium containing fungicides Proline EC 250 (Bayer Crop Science; active ingredient prothioconazole, azole group of fungicides, 0.0125 µg /ml), Cantus WDG (BASF Canada Inc; active ingredient boscalid, anilid group of fungicides, boscalid, 2000 µg/ml), Chipco green 75 WG (Bayer Crop Science; active ingredient iprodione, dicarboximide group of fungicides, iprodione, 250 µg/ml), or Teldor WG 50 (Bayer Crop Science; active ingredient fenhexamid; hydroxyanilide group of fungicides, fenhexamid, 7500 µg/ml); hypoxia inducing agent cobalt chloride (Merck, NJ; $CoCl_2$ 2.5 mM); cell wall stressors SDS (0.05 %) or caffeine (0.1 %). The optimum concentration of Proline fungicide and $CoCl_2$ was selected based on the screening of *C. rosea* to these compounds on CZ plates. The concentration of other fungicides and cell wall stress inducers used in this study is described in our previously published results (Dubey et al., 2014a, 2016). Colony diameter was measured four dpi at 20 °C. Agar plugs of *C. rosea* strains were inoculated on microscope slides with CZ medium supplemented with prothioconazole for microscopy observation of colony morphology. The mycelial edge of the colonies was photographed using a Leica DM5500M Microscope equipped with a Leica DFC360FX digital camera (Wetzlar, Germany).

Antagonistic behavior against the fungal hosts, *B. cinerea, F. graminearum* and *R. solani* was tested using an *in vitro* dual culture plate confrontation assay on PDA medium as described before (Dubey et al., 2014a, 2014b, 2016). The growth of *B. cinerea, F. graminearum* and *R. solani* was measured daily until their mycelial front touched the *C. rosea* mycelial front. The growth of *C. rosea* strains over the fungal hosts was measured until the fungus reached another side of the plate. The plate confrontation assay was performed in four biological replicates.

The biocontrol ability of the *C. rosea* strains against *F. graminearum* was evaluated using a fusarium foot rot assay (Dubey et al., 2020; Knudsen et al., 1995). In brief, surface sterilised wheat seeds were

treated with *C. rosea* conidia (1e+07 conidia/ml) in sterile water, sown in moistened sand, and kept in a growth chamber after pathogen inoculation (Dubey et al., 2016, 2014b). Plants were harvested three weeks post-inoculation, and disease symptoms were scored on a 0–4 scale, as described before (Dubey et al., 2014b; Knudsen et al., 1995). The experiment was performed in five biological replicates, with 15 plants in each replicate.

2.9. RNA sequencing

The transcriptome of *C. rosea* WT and Δ*sre1* strains was analysed in submerged liquid CZ medium and CZ medium amended with prothioconazole (active ingredients of Proline fungicide). Conidia of *C. rosea* strains were pre-cultivated for two days in 100 ml flasks containing 20 ml liquid CZ medium on a rotary shaker (100 rpm) at 25 °C after which the growth medium was amended directly with 0.03 ppm prothioconazole. After 24 h of incubation, fungal mycelia were harvested, washed in distilled water, frozen in liquid nitrogen and stored at −80 °C. The experiment was performed with four biological replicates. RNA extraction was done using the Qiagen RNeasy kit following the manufacturer's protocol (Qiagen, Hilden, Germany). After DNaseI (Fermentas, St. Leon-Rot, Germany) treatment, the RNA quality was analysed using a 2100 Bioanalyzer Instrument (Agilent Technologies, Santa Clara, CA), and concentration was measured using a Qubit fluorometer (Life Technologies, Carlsbad, CA). For mRNA sequencing, the total RNA was sent for library preparation and paired-end sequencing at the National Genomics Infrastructure (NGI), Uppsala, Sweden. Sequencing libraries were prepared using the TruSeq stranded mRNA library preparation kit (Illumina Inc. San Diego, CA), including polyA selection according to the manufacturer's protocol (Illumina Inc. San Diego, CA). The mRNA libraries were sequenced on one NovaSeq SP flowcell with a 2×150 setup using the Illumina NovaSeq6000 system at the SNP&SEQ Technology Platform, Uppsala, Sweden.

For RNAseq analysis, the raw reads underwent adapter removal and quality trimming with the BBDuk tool from BBmap v. 38.9 (with options "ktrim=r k=23 mink=11 hdist=1 tpe tbo qtrim=r trimq=10 maq=10") (Bushnell, 2019), and quality was checked with FastQC v. 0.11.9 (Andrews, 2010). The clean reads were mapped to the genome of *C. rosea* IK726 (GCA_902827195.2) using STAR v. 2.7.9a with default parameters (Dobin et al., 2013). The number of reads mapping to each gene was counted using featureCounts v. 2.0.1 (with options "-p -O –fraction -g Parent -t exon -s 2") (Liao et al., 2014). The differentially expressed genes were then determined using the R package DESeq2 (Love et al., 2014) with a maximum FDR-adjusted p-value of 0.05 and a threshold on absolute log2(FC) 1.

Gene ontology enrichment was done by performing one-tailed Fisher exact tests with an FDR threshold of 0.05 using BLAST2GO v. 5.2.5 (Conesa et al., 2005). The annotation of the *C. rosea* genome used for the analysis was the same one described in Piombo et al. (2021). Furthermore, differentially expressed genes involved in respiration, iron ion binding, sterol metabolism, and cytochrome P450 genes were predicted using the annotation of Piombo et al. (2021). ABC and MFS transporters were also identified, and they were assigned a class depending on the prediction in Broberg et al. (2021). The proteins encoded by these genes of interest were compared with the fungal section of the NCBI non-redundant database using BLAST (Altschul et al., 1990).

2.10. Gene expression analysis by RT-qPCR

Total RNA isolated from *C. rosea* WT and Δ*sre1* strains was used for gene expression analysis using RT-qPCR. After DNAse (Fermentas, St. Leon-Rot, Germany) treatment, total RNAs was reverse transcribed using the iScript cDNA synthesis kit (Bio-Rad, Hercules, CA, United States). Transcript levels were quantified using the SYBR Green PCR Master Mix (Fermentas, St. Leon-Rot, Germany) and gene-specific primer (**Supplementary Table 2)** in CFX96 real-time PCR detection system (Bio-Rad, Hercules, CA). For gene expression analysis, relative expression levels for the target gene in relation to actin gene was calculated from threshold cycle (Ct) values using the $2^{-\Delta\Delta Ct}$ method (Livak and Schmittgen, 2001). Gene expression analysis was conducted in four biological replicates, each with two technical replicates.

2.11. Statistical analysis

Analysis of variance (ANOVA) was performed on gene expression and phenotype data using a general linear model approach implemented in Statistica version 13 (TIBCO Software Inc., Palo Alto, CA). Pairwise comparisons were made using the Fisher's exact test at the 95 % significance level. The students' *t-test* was also performed on heterologous gene expression data.

3. Results

3.1. Identification and sequence analysis of SREBPs, INSIG and SCAP in *C. rosea*

Analysis of the *C. rosea* strain IK726 genome (Broberg et al., 2018; Karlsson et al., 2015) identified two genes predicted to encode SREBPs (CRV2T00000933_1, named *sre1*; CRV2T00003323_1, named *sre2*), one gene each encoding for INSIG (CRV2T00010728_1, named *insig*), and SCAP (CRV2T00000306_1, named *scap*). *sre1* encodes for a protein with 999 aa, with a predicted bHLH domain (PF00010, IPR011598) with a tyrosine (Y) residue unique to SREBP at the N-terminus, a domain of unknown function DUF2014 (PF09427) at C terminus and two transmembrane helices. SRE2 has 328 residues and lacks the DUF2014 domain and transmembrane helices (**Supplementary Figure 2**). The characteristics of these proteins are presented in Table 1. Like previously characterized SRE sequences, the bHLH domain of *C. rosea* SRE proteins contains conserved HNxxExxYR and KxxxLxxAxxYxxxL motifs in the basic and helix regions, while the loop region is highly variable (Fig. 1**A**). A phylogenetic analysis using the bHLH domain of selected SREBP proteins (Chung et al., 2019) showed that *C. rosea* SRE1 belongs to Sordariomycetes SRE clade 1 (also called SRE clade A; Ruan et al., 2019), while SRE2 is external to both clade one and clade two (also called clade B; Ruan et al., 2019) (Fig. 1**B**).

The putative INSIG homolog (CRV2T00010728_1) in *C. rosea* is predicted to consist of 407 residues and contains the INSIG superfamily domain (PF07281, IPR025929) at aa position 165–392 and six transmembrane helices between aa position 160 and 388. The *C. rosea* SCAP is composed of 1127 aa with a SCAP family domain (IPR030225) consisting of sterol sensing domain (SSD; IPR000731, PF12349), eight transmembrane helices spanning between 36 aa – 936 aa, and two WD40 repeat motif (IPR001680) between 554 aa – 593 aa and 659 aa – 730 aa, mediating protein-protein interactions (Table 1**; Supplementary Figure 2**). The phylogenetic tree obtained by comparing the *C. rosea* SCAP and INSIG proteins to the sequences used by Chung et al. (2019) showed that the phylogenetic position of *C. rosea* SCAP and INSIG are congruent with the species phylogeny (Karlsson et al., 2015; **Supplementary Figure 3**).

3.2. Distribution of SREBP genes in Hypocreales

To investigate the distribution of SREBP, INSIG and SCAP genes among fungal species from the order Hypocreales, we searched 40 fungal genomes representing plant-pathogenic, insect-pathogenic, mycoparasitic and nematode-parasitic lifestyles (**Supplementary Table 1**). SRE1 homologues were identified in all analysed species except insect pathogens *Escovopsis weberi* and *Cordyceps militaris*. At the same time, the gene coding for SRE2 is variably distributed, from one gene among the fungi with mycoparasitic and nematophagous lifestyles to three genes in plant pathogenic lifestyles such as *Claviceps purpurea*. Interestingly, the SRE2 gene is absent in specific insect pathogenic fungi

Table 1
Characteristics of putative SREBPs, INSIG and SCAP protein in *C. rosea*.

Name	Transcript ID	Length of genomic sequence	No of introns	Protein length	Transmembrane helices	Domain
SRE1	CRV2T00000933	3054	1	999 aa	2	DUF2014 (239 aa – 313 aa) bHLH (581 aa – 845 aa)
SRE2	CRV2T00003323	984	0	328 aa	0	bHLH (210 aa – 316 aa)
INSIG	CRV2T00010728	1292	2	407 aa	6	INSIG superfamily (165–392 aa)
SCAP	CRV2T000003061	3563	2	1127 aa	8	SCAP family (7 aa – 699 aa) WD40 (554 aa – 563 aa; 606 aa – 640 aa); SSD (318 – 457)

(for example, *Beauveria bassiana* and *Cordyceps militaris*) that belong to the family Cordycipitaceae, but other insect pathogens such as *Metarhizium anisopliae* and *M. anisopliae* from Clavicipitaceae family contain two SRE2 genes (**Supplementary Table 3).** The gene copy number of genes coding for SCAP and INSIG are conserved among the species analysed in this study except for *Lecanicillium lecanii* and *Torrubiella hemipterigena*, which lack a SCAP homologue, and *Stachybotrys chartarum* lacking INSIG (**Supplementary Table 3).**

3.3. SRE1, but not SRE2, interacts with SCAP

To investigate the physical interaction between SREBP and SCAP, we used Y2H, a well-established method to study protein-protein interactions (Brückner et al., 2009). Yeast strains co-transformed with SRE1 and SCAP were able to grow on the auxotrophic selection plates (-His, -Ade, -Leu, -Trp), while yeast strains co-transformed with SRE2 and SCAP failed to grow on selection plates. The results from the Y2H assay suggested a physical interaction between SRE1 and SCAP but not between SRE2 and SCAP (Fig. 2**A).**

3.4. Overexpression of C. rosea sre1 in Saccharomyces cerevisiae enhanced tolerance to prothioconazole

To investigate the role of *C. rosea* SRE1 and SRE2 in azole tolerance, we generated *S. cerevisiae* strains overexpressing *C. rosea sre1* (SRE1 OE) and *sre2* (SRE2 OE). An *S. cerevisiae* strain transformed with an empty vector (EV) was used as a control. The *S. cerevisiae* genome lacks SREBP, and sterol synthesis is regulated by a typical Gal4-type zinc finger transcription factor named Upc2, which differs from SREBP in protein structure. The tolerance of SRE1 OE and SRE2 OE to prothioconazole (the active ingredient of fungicide formulation Proline, which inhibits ergosterol biosynthesis) was determined by measuring their growth rates in SC -Ura medium supplemented with 1.5 ppm prothioconazole. A significant 35 % and 30 % ($P = 0.001$) increase in growth of the *S. cerevisiae* SRE1 OE strain was found compared to the EV control at 16 hpi and 20 hpi, respectively (Fig. 2**B**). In contrast, the *S. cerevisiae* SRE2 OE strain showed no significant difference in growth compared to the EV control at the tested time points (Fig. 2**C**). No significant differences ($P \geq 0.061$) in growth between SRE1 OE strain or SRE2 OE strain and EV control was observed, showing that the overexpression of both SREBPs does not negatively impact the growth of *S. cerevisiae* (Fig. 2**C**).

Since overexpression of *C. rosea* SRE1 in *S. cerevisiae* could enhance the tolerance to prothioconazole, we overexpressed this gene in *S. cerevisiae UPC2* knock-out strain (Δupc*2*) background (SRE1 upc2) to investigate whether SRE1 is a functional analogue to Upc2. Since *S. cerevisiae* SRE1 upc2 strain showed a reduced growth rate ($P = 0.001$) compared to that of the empty vector (EV upc2) control (**Supplementary Figure 4**), the growth rate of SRE1 upc2 and EV upc2 in prothioconazole was normalized to the growth rate in control SC -Ura medium. The result showed no significant differences ($P \geq 0.21$) in the normalized growth rate between the SRE1 upc2 strain and empty EV upc2 (Fig. 2**D**). The reduced growth of the upc2 deletion mutant overexpressing *C. rosea* SRE1 compared to the EV control is intriguing, and more experimental evidence is needed to provide a plausible explanation for this phenotype".

3.5. Generation of sre deletion and complementation strains

To characterize the biological role of SRE1 and SRE2 in *C. rosea*, *sre1* and *sre2* deletion strains were generated by replacing the genes with the hygromycin resistance gene cassette hygB through ATMT **(Supplementary Figure 1**). Successful gene replacement in hygromycin-resistant transformants was confirmed by PCR using primers following the procedure described previously (Dubey et al., 2012). The expected size of PCR fragments was amplified in Δ*sre1* and Δ*sre2* strains, while no amplification was observed in the WT (**Supplementary Figure 1**). Furthermore, RT-PCR experiments using primers specific to the *sre1* and *sre2* sequences demonstrated the complete loss of *sre1* and *sre2* transcripts in each mutant, while expression of *sre1* and *sre2* was detected in the WT (**Supplementary Figure 1**). The Δ*sre1* strain was complemented with *sre1*. Successful integration of the complementation cassette in mitotically stable mutants was confirmed by PCR amplification of the geneticin-resistant selection cassette (**Supplementary Figure 1**). RT-PCR from randomly selected geneticin positive Δ*sre1* strains using *sre1*-specific primer pairs demonstrated restored *sre1* transcription in Δ*sre1* complemented (Δ*sre1*+) strains. No transcripts were detected in the parental deletion strains (**Supplementary Figure 1**).

3.6. Deletion of sre1 affects C. rosea tolerance to fungicides and hypoxia

No differences in growth rate were detected between the deletion and WT strains on the PDA or CZ medium. The role of SRE in fungicide tolerance was investigated by comparing the growth rate of SRE deletion and WT strains on a CZ medium amended with Proline fungicide (active ingredient prothioconazole, demethylation [ERG11 C14-demethylase] inhibitor in sterol biosynthesis), Teldor fungicide (active ingredient fenhexamid, 3-keto reductase [ERG27] inhibitor in sterol biosynthesis), Cantus fungicide (active ingredient boscalid, succinate-dehydrogenase [SDH] inhibitor in respiration) or Chipco Green fungicide (active ingredient iprodione, mitogen-activated protein [MAP]/histidine-kinase inhibitor in osmotic signal transduction). The growth rate of the Δ*sre1* strains was 51 % and 22 % lower ($P < 0.001$) than the WT growth rate on CZ amended with Proline fungicide or Cantus fungicide, respectively. At the same time, no significant difference in growth rate was found between the deletion and WT strains on CZ amended with Chipco Green or Teldor fungicides (Fig. 3**A**). The complementation strain Δ*sre1*+ showed complete restoration of the growth rate phenotypes observed in Δ*sre1*. Microscopic observation of *C. rosea* colonies showed a deformed mycelial front of Δ*sre1* strain on PDA supplemented with Proline fungicide (**Supplementary Figure 5**).

To determine if the deletion of *sre* affects *C. rosea*'s ability to tolerate hypoxia, the growth rate of the WT and *sre* deletion strains were compared on a CZ medium amended with hypoxia-mimicking agent $CoCl_2$ (Lee et al., 2007). The Δ*sre1* strains displayed a 17 % reduced growth rate ($P < 0.01$) on the $CoCl_2$-supplemented CZ medium compared to the WT (Fig. 3**A**). Since SREBP regulates ergosterol biosynthesis, we hypothesized that deleting *sre1* and *sre2* would influence *C. rosea* cell wall and membrane integrity. To evaluate this, *C. rosea*

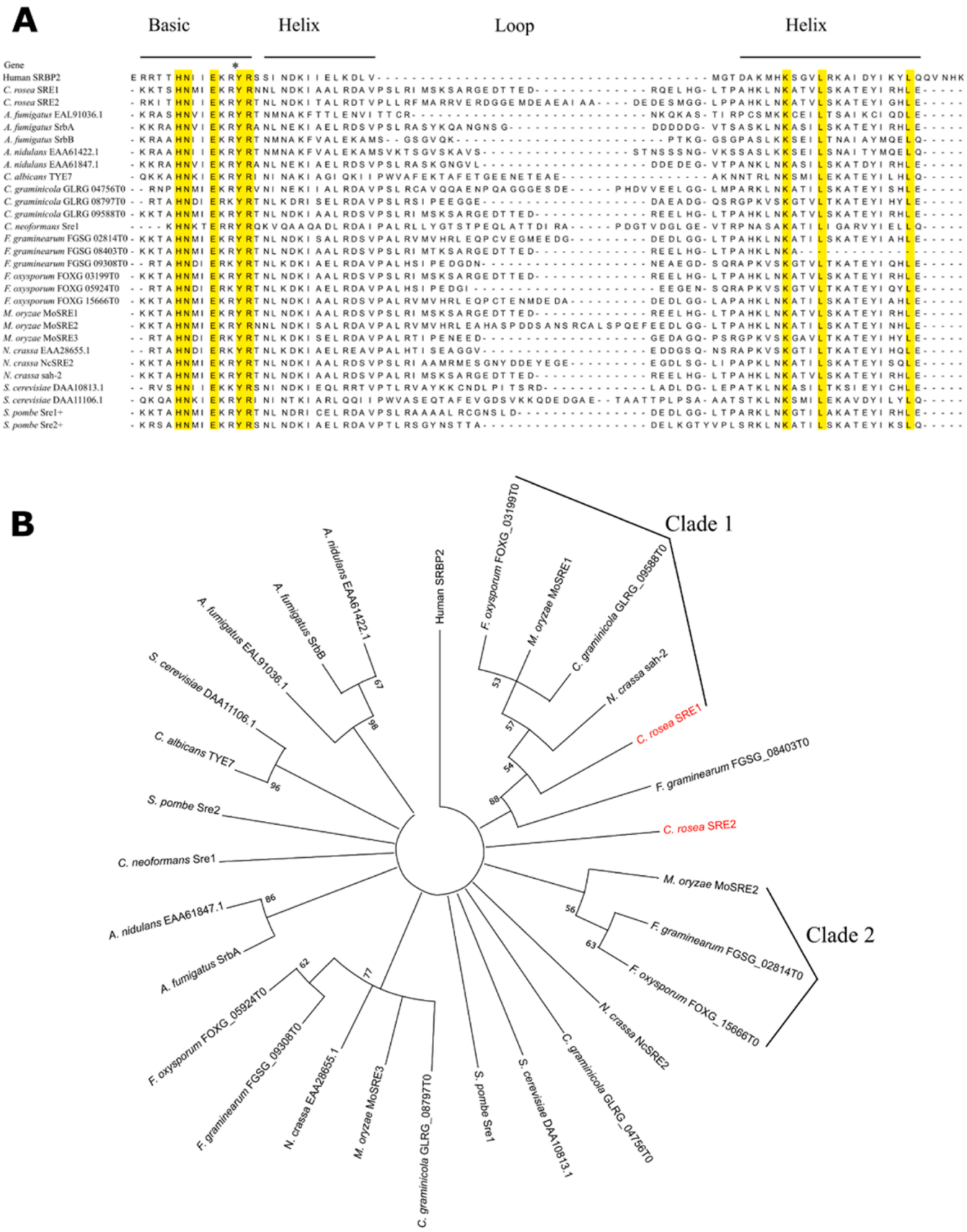

Fig. 1. Alignment of the BHLH domain of SRE proteins (**A**) and phylogenetic tree based upon the same sequences (**B**). Besides *C. rosea* SRE1 and SRE2, the proteins included are considered in the work of Chung et al. (2019), which also defines the two shown clades. The trees were obtained with IQ-TREE v. 2.1.3 (Minh et al., 2020). The SRE tree nodes with bootstrap values less than 50 % were condensed through MEGA v. 10.0.5.

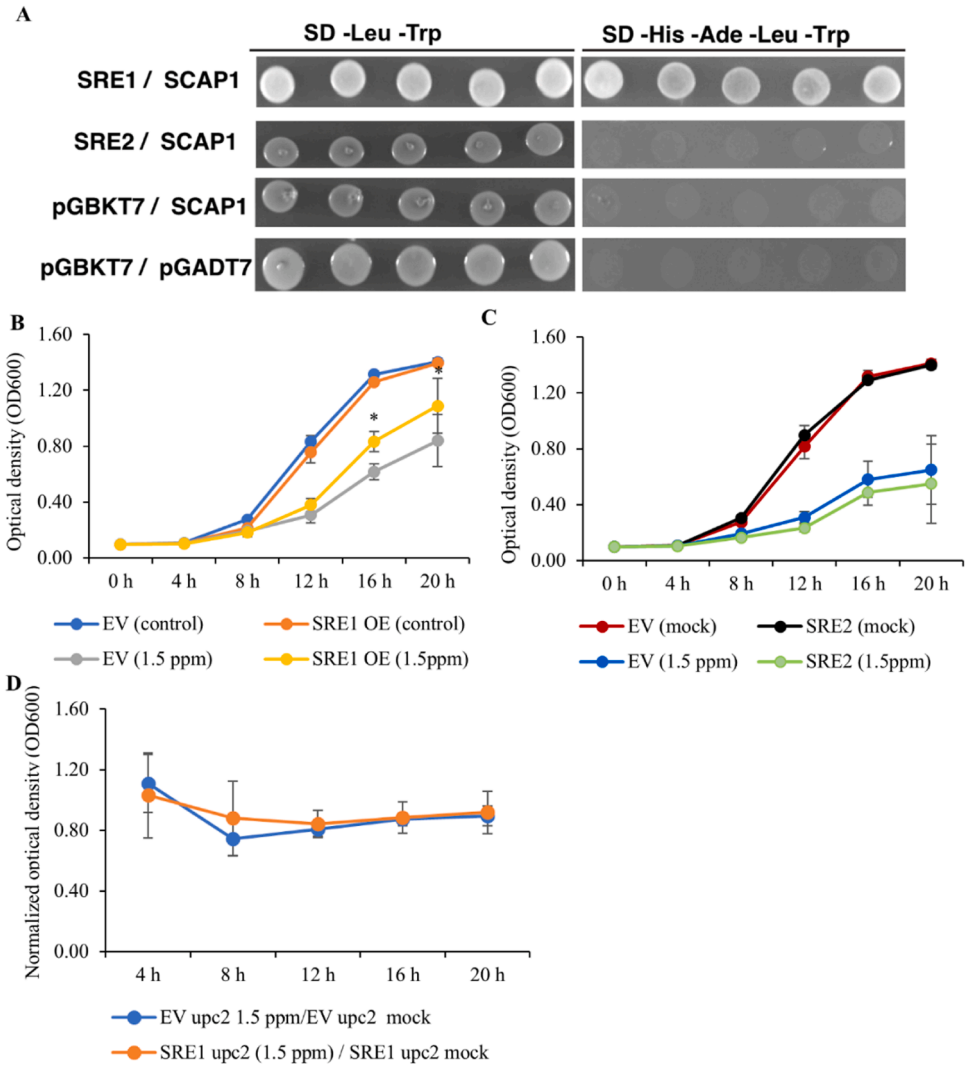

Fig. 2. Analysis of the *sre1* and *sre2* genes in *Saccharomyces cerevisiae*. **A**: Yeast-two-hybrid assay between SRE1 or SRE2 (used as a bait in pGBKT7 vector) and SCAP (used as a prey in pGADT7 vector). Growth of yeast cells on SD-4 (-His, -Ade, -Leu, -Trp) selective media represents protein-protein interaction and growth on SD-2 (-Leu, -Trp) media confirms yeast transformation. Yeast transformed with the empty vectors were used as negative controls. **B**: Growth of *S. cerevisiae* overexpressing *sre1* upon exposure to 1.5 ppm prothioconazole. **C**: Growth of *S. cerevisiae* overexpressing *sre2* upon exposure to 1.5 ppm prothioconazole. **D**: Growth of *S. cerevisiae upc2* mutants complemented with either *sre1* or *sre2* upon exposure to 1.5 ppm prothioconazole. *S. cerevisiae* strain transformed with the empty pYES-2 vector (EV) and grown in an equal volume of 50 % DMSO was used as controls. The values at the y-axis represent the ratio of *S. cerevisiae* growth in the presence of prothioconazole to the growth under control conditions (50 % DMSO). Asterisks denote statistically significant differences based on a t-test ($p < 0.05$). Error bars represent standard deviation based on six biological replicates.

strains were grown on CZ supplemented with cell wall stress inducers caffeine or SDS, which has been used as criteria for testing cell wall integrity in fungi and yeasts (Klis et al., 2002; Kuranda et al., 2006; Nunez et al., 2008). The growth rate of Δ*sre1* strains was increased by 17 % ($P < 0.001$) on Caffeine; however, there was a 12 % decrease ($P \leq 0.007$) in the SDS medium (Fig. 3**A**). The complementation strain Δ*sre1*+ showed complete restoration of the growth rate phenotypes observed in Δ*sre1*. No differences in mycelial growth rate were detected between the WT and Δ*sre2* deletion strains on these media (**Supplementary Figure 6 A**).

3.7. Deletion of sre1 altered C. rosea antagonism

An in *vitro* dual culture plate confrotation assay was used to test whether deletion of *sre1* or *sre2* affected the antagonistic ability of *C. rosea* against the fungal hosts *B. cinerea*, *F. graminearum* and *R. solani*. During dual-culture interactions, *C. rosea* initially reduces the mycelial growth of fungal hosts and then, after mycelial contact, starts to overgrow and conidiate on the mycelia of the fungal hosts. Three dpi, *B. cinerea* exhibited a significant ($P \leq 0.036$) 17 % decrease in growth rate during a confrontation with Δ*sre1* strains compared to the WT (Fig. 3**B**), indicating increased antagonistic ability of Δ*sre1* against *B. cinerea*. However, no differences in the growth rate of *F. graminearum* and *R. solani* were recorded during the same conditions. Similarly, no differences in growth rate between *C. rosea* WT and deletion strains were measured during the confrontation with the fungal hosts. After the mycelial contact, *C. rosea* strains and the fungal hosts were allowed to interact with each other for ten days. The growth rate of Δ*sre1* strains was 20 % higher ($P \leq 0.012$) on *B. cinerea* mycelium (overgrowth rate) compared to the growth rate of WT (Fig. 3**C**). In contrast, overgrowth on *R. solani* was reduced by 20 % ($P < 0.001$); however, overgrowth on *F. graminearum* was not compromised (Fig. 3**C**). Like *in vitro* antagonism tests, a bioassay for biocontrol of fusarium foot rot diseases on wheat caused by *F. graminearum* showed no significant difference in biocontrol ability between the WT and the Δ*sre1* strain. Moreover, no differences in antagonism and biocontrol ability were found between the WT and

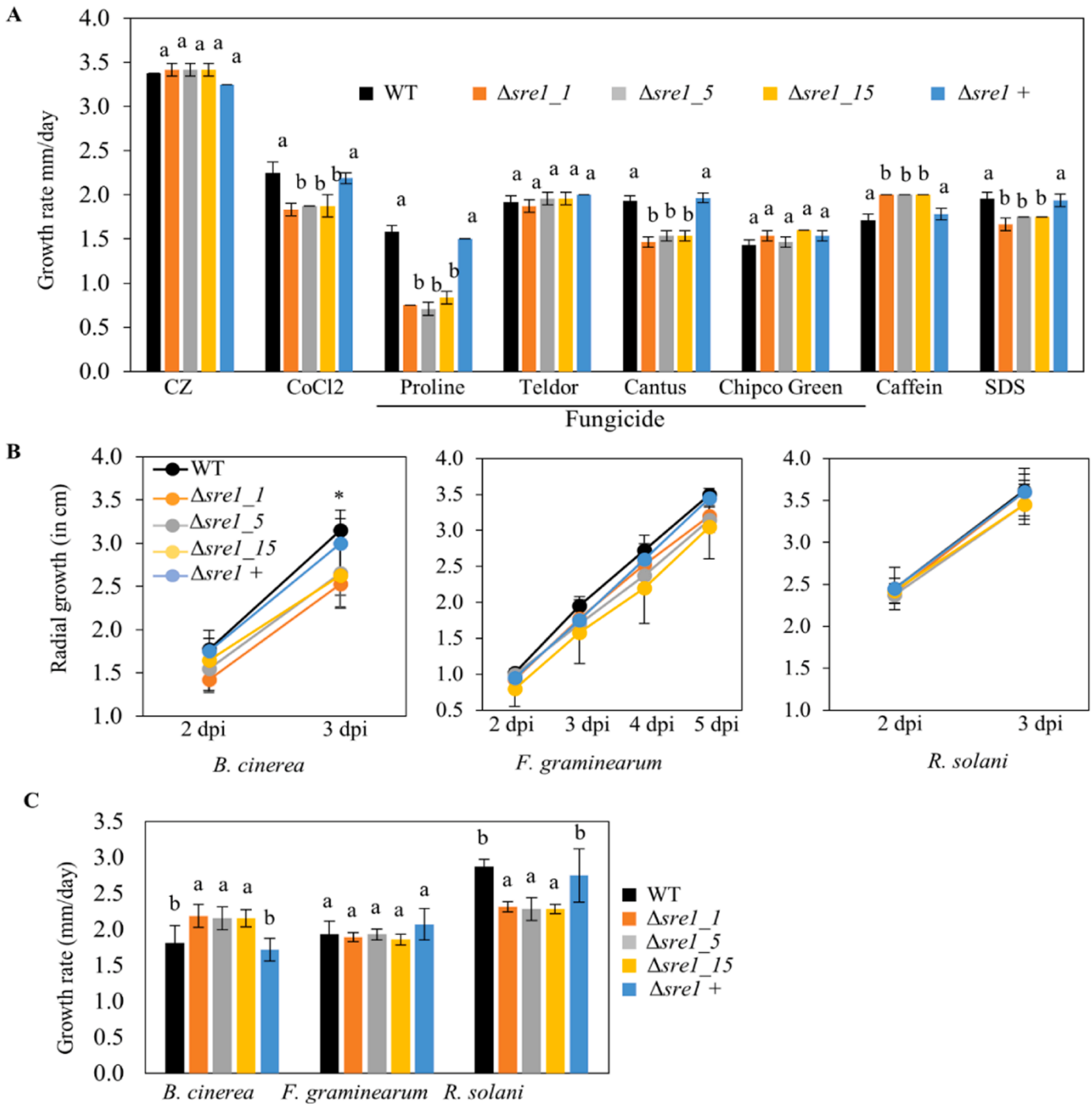

Fig. 3. Phenotypic characterizations of *C. rosea* WT, *sre1* deletion and complementation strains. **A**: Growth rate of *C. rosea* WT or Δ*sre1* on czapek-dox medium (CZ) or CZ medium supplemented with fungicides Proline (0.0125 μg /ml), Teldor (7500 μg/ml), Cantus (2000 μg/ml), Chipco Green (250 μg/ml), hypoxia mimicking agent CoCl2 (2.5 mM) and cell wall stressors SDS (0.05 %) and Caffeine (0.1 %). Strains were inoculated on a solid agar medium and incubated at 20°C, and the growth rate was recorded five days post-inoculation. The experiments were carried out in three biological replicates. Different letters indicate statistically significant differences ($P \leq 0.05$) within experiments based on the Fisher exact test at the 95 % significance level. **B**: Plate confrontation assay to measure the antagonistic ability of *C. rosea* strains against the fungal hosts *B. cinerea*, *F. graminearum* and *R. solani.* Agar plugs of *C. rosea* strains and the fungal hosts were inoculated on opposite sides in 9 cm diameter agar plates and incubated at 20°C. Radial growth of *B. cinerea*, *F. graminearum*, and *R. solani* were recorded daily during growth in dual culture with *C. rosea* WT and Δ*sre1*. The experiments were carried out in four biological replicates. Different letters indicate statistically significant differences ($P \leq 0.05$) within experiments based on Fisher's exact test at the 95 % significance level. **C**: The mycoparasitic ability of *C. rosea* strains was analyzed by measuring their growth rate over the fungal hosts in a dual culture assay. The Δ*sre1* strains showed an enhanced ability to grow on *B. cinerea* and a reduced ability to grow on *R. soalni.* The growth of *C. rosea* strains on the fungal hosts was measured from the point of mycelial contact. The experiment was performed in four replicates. Different letters indicate statistically significant differences based on Fisher's exact test at the 95 % significance level.

Δ*sre2* (**Supplementary Figure 6B, 6 C**).

3.8. Transcriptome analysis of C. rosea WT and sre1 deletion strain

To dissect the SREBP-mediated gene regulatory network in *C. rosea* and understand the underlying mechanism of impaired Δ*sre1* phenotypes, the transcriptome of *C. rosea* WT and Δ*sre1* was compared in the submerged liquid CZ without or with prothioconazole (CZ + Pro) treatment conditions. The sequencing obtained, on average, 30.9 million reads per sample (**Supplementary Table 4**). The analysis identified 2145 genes commonly upregulated in Δ*sre1* for both treatments compared to the WT, while 544 and 580 genes were uniquely upregulated under CZ and CZ + Pro treatment, respectively. Similarly, 2480 genes were downregulated in both treatments, while 572 and 704 were downregulated in only one treatment (Fig. 4**A, Supplementary Table 5** The upregulated genes in CZ and CZ + Pro were significantly enriched in 282 and 352 biological processes GO terms, respectively **(Supplementary Table 6**). Among the enriched GO terms category biological process, a higher number was related to metabolic and biosynthetic processes, followed by membrane transport and respiration (Fig. 4**B**). Meanwhile, the number of GO terms associated with aerobic respiration, iron homeostasis, lipid biosynthesis, and pigment biosynthesis were reduced **(Supplementary Figure 7 Supplementary Table 6**).

To study if deletion of *sre1* affected regulatory feedback loops that influence expression levels of SREBP-associated genes, the expression of *sre2*, *scap* and *insig* was examined by comparing their expression pattern in *C. rosea* WT and Δ*sre1*. The deletion of *sre1* resulted in the downregulation of *sre2,* while the expression of *scap* and *insig* was unaffected (Table 2). This suggests that the expression of *sre2* is correlated with *sre1*, while the expression of *insig* and *scap* is independent of the expression of SREBP in *C. rosea*.

3.9. Deletion of sre1 triggered transcriptional reprogramming of genes associated with lipid metabolism, aerobic respiration and xenobiotic tolerance

Since SREBPs are shown to regulate expression patterns of genes associated with lipid homeostasis, tolerance to hypoxia and drug tolerance, the transcriptome of *C. rosea* strains was further analysed, focusing on genes involved in these processes. Our analysis showed downregulation of monooxygenase coding gene *erg1* under both conditions, which catalyses the first step in the ergosterol biosynthetic pathway, in Δ*sre1* compared to the WT. Intriguingly, six mevalonate pathway genes (*erg10*, *erg13*, *hmgr*, *idi1*, *erg20*, *erg9*) that biosynthesize precursors of ergosterol and carotenoid were significantly upregulated (Fig. 5). Similarly, *crtYB* and *crtI,* part of the carotenoid biosynthetic pathway, and *erg7*, *erg11* and *erg26*, part of ergosterol biosynthetic pathways, were upregulated. In addition, we identified 51 DEGs (29 upregulated and 22 downregulated) in Δ*sre1* compared to the WT with a putative role in lipid biosynthetic and metabolic processes (**Supplementary Table 7**).

We analysed the expression patterns of genes associated with aerobic respiration, such as those involved in glycolysis, tricarboxylic acid (TCA) cycle and mitochondrial electron transport. Seven genes out of ten involved in glycolysis were downregulated in the Δ*sre1* compared to the WT under both conditions (Fig. 6). Similarly, a gene coding for peroxisomal malate dehydrogenase MDH3, which catalyses the conversion of malate to oxaloacetate in the glyoxylate cycle, an anabolic variant of the TCA cycle, is downregulated in Δ*sre1* compared to the WT. The alcohol dehydrogenase (ADH1) gene responsible for catalysing the reduction of acetaldehyde to ethanol during fermentation is also downregulated. In contrast to glycolysis, TCA cycle genes were upregulated in Δ*sre1* except for citrate synthase gene *cit3,* which catalyses the first step of the TCA cycle, performing the condensation of acetyl-CoA with oxaloacetate to form citrate (Fig. 6**)**. Similarly, 12 genes associated with the electron transport chain and aerobic respiration in mitochondria were upregulated. This includes genes coding for subunits of succinate dehydrogenase (ubiquinone), ubiquinol cytochrome C reductase, cytochrome b-c1 complex, CHCH domain protein and mitochondrial trans-2-enoyl-CoA reductase (Fig. 6). However, a gene (CRV2T00003883_1) coding for 2-hexaprenyl-6-methoxy-1,4-benzoquinone methyltransferase, required for ubiquinone biosynthesis, was found to be downregulated.

Table 2
Expression analysis of *sre2*, *insig* and *scap* genes in the *sre1* deletion strain compared to *C. rosea* WT. Values in bold indicate significant differential expression with FDR < 0.05.

Gene name	Log2(FC) on CZ	Log2(FC) on CZ + Pro
sre2	**−2.57**	**−2.46**
scap	0.15	−0.12
insig	0.92	0.67

Our analysis showed 38 DEGs (17 upregulated, 21 downregulated) related to iron homeostasis, which plays an essential role in cellular respiration and oxygen transport in fungi (Blatzer et al., 2011). This includes 13 genes coding for heme peroxidase, iron permease FTR1 family protein, siderophore iron transporter mirb protein, FeS biogenesis, and iron-sulfur cluster assembly protein (Table 3). We also identified 13 differentially expressed MFS transporter genes with high similarity with siderophore-iron transporter 1 *Sit1* and *Str1*, ferri-siderophore transporter *MirB* and Fusarium iron-related protein *Fir1* (Table 3**)**.

To test the role of membrane transporters in fungicide tolerance in *C. rosea*, we compared the expression pattern of membrane transporter genes between Δ*sre1* and the WT strains. We focused our analysis on MFS (major facilitator superfamily) transporters and ABC (ATP-binding cassette) transporter genes, which are considered crucial for their role in fungicide tolerance in *C. rosea* (Broberg et al., 2018; Dubey et al., 2014a, 2016; Funck Jensen et al., 2021; Karlsson et al., 2015). Gene expression analysis identified 215 MFS transporter genes differentially expressed in Δ*sre1* compared to the WT. Among these, 52 (34 upregulated, 18 downregulated) were classified as putative drug transporters with potential roles in fungicide and xenobiotic tolerance (Table 4,

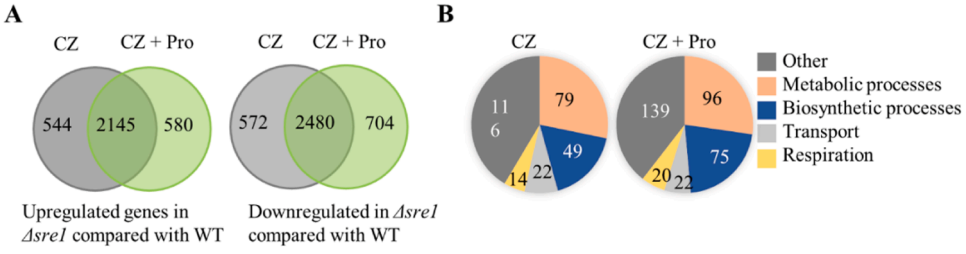

Fig. 4. A: Number of genes differentially expressed in Δ*sre1* in Czapek-dox medium (CZ) and CZ medium supplemented with prothioconazole (CZ + Pro), compared to the WT. All differentially expressed genes were determined using DESeq2 (Love et al., 2014) with an adjusted p-value of ≤ 0.05 and log2FC threshold of 1.**B:** Number of GO terms enriched in the genes upregulated in Δ*sre1* compared to *C. rosea* WT. GO enrichment was determined with a one-tailed Fisher exact test with an FDR of ≤ 0.05 using BLAST2GO v. 5.2.5 (Conesa et al., 2005). The numbers in the pie chart indicate Go terms enriched in Δ*sre1* strains compared with the WT.

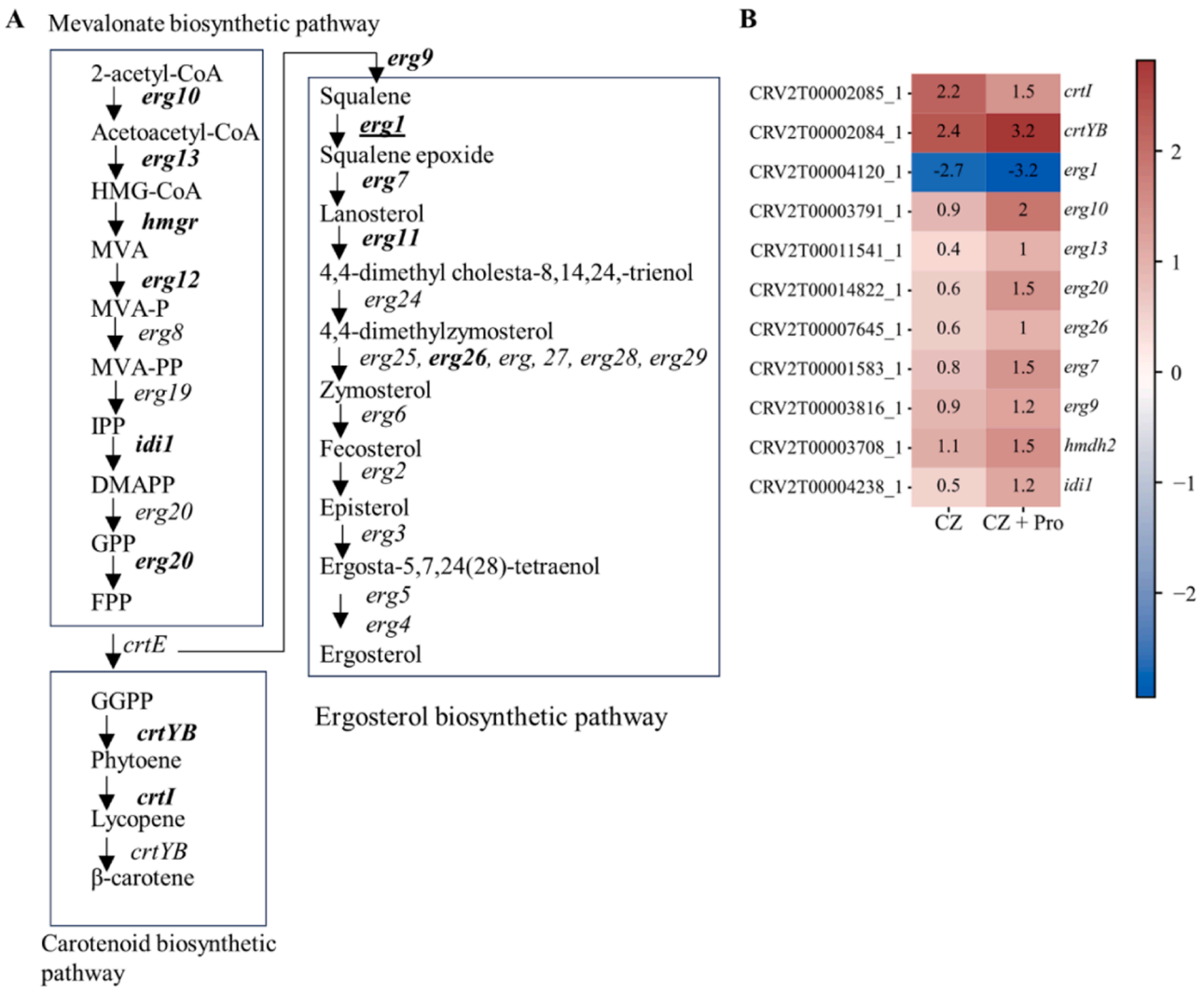

Fig. 5. A: Ergosterol biosynthetic genes differentially expressed in Δ*sre1* compared to the WT. Gene significantly upregulated in Δ*sre1* compared to the WT are indicated with bold letters. Gene (*erg1*) downregulated is indicated with bold and underlined letters. **B**. Heatmap showing the log2(FC) of gene expression in Δ*sre1* compared to the WT in CZ and CZ supplemented with prothioconazole (CZ + Pro). All differentially expressed genes were determined using DESeq2 (Love et al., 2014) with an adjusted p-value of ≤ 0.05 and log2FC threshold of 1. Red and blue colours represent up-regulated and down-regulated genes, respectively. HMG-CoA, 3-hydroxy-3-methylglutaryl-CoA; MVA, mevalonate; MVA-P, mevalonate-5-phosphate; MVA-PP, mevalonate-5-pyrophosphate; IPP, isopentenyl-pyrophosphate; DMAPP, dimethylallyl-pyrophosphate; GPP, geranyl-pyrophosphate; FPP, farnesyl-pyrophosphate; GGPP, geranylgeranyl-pyrophosphate. crtI, Phytoene desaturase; crtYB, Phytoene synthase; ERG1, Squalene monooxygenase; ERG10, Acetyl-CoA acetyltransferase-like protein; ERG12, Mevalonate kinase; ERG13, Hydroxymethylglutaryl- synthase; ERG20, Farnesyl pyrophosphate synthase; ERG26, Sterol-4-alpha-carboxylate 3-dehydrogenase; ERG7, Terpene cyclase; ERG9, Squalene synthase-like protein; HMDH2, Hmg CoA reductase; IDI1, Isopentenyl-diphosphate delta-isomerase.

Supplementary Table 7). This includes genes showing high similarity with MFS transporters *mfs1, qdr2* and *qdr3*, which have been characterized for their role in drug, mycotoxins and fungicide tolerance (Liu et al., 2012; Qadri et al., 2022; Saier et al., 2021). Similarly, 49 ABC transporter genes (30 upregulated and 19 downregulated) were differentially expressed in Δ*sre1* compared to the WT. This includes 15 genes from the pleiotropic drug resistance protein (PDR) family ABC-G, seven from multidrug resistance-associated protein (MRP) family ABC-C and ten from multidrug resistance protein (MDR) family ABC- B (Table 4, **Supplementary Table 7**). The expression pattern of genes coding for Cytochrome p450 (CYP), a heme-containing protein involved in xenobiotic metabolism in fungi, was also analysed (Chen et al., 2014; Manikandan and Nagini, 2018). Our analysis identified 75 differentially expressed (31 upregulated and 44 downregulated) CYP450 genes in Δ*sre1* compared to the WT (**Supplementary Table 7**). These include CYP51 gene coding for eburicol 14-alpha-demethylase-like protein and isotrichodermin C-15 hydroxylase, critical in the ergosterol biosynthesis pathway and secondary metabolite production.

3.10. Antagonism-responsive genes were downregulated in Δsre1 strain

We used transcriptome data from previous studies during *C. rosea* interactions with plant pathogenic fungal hosts *B. cinerea*, *F. graminearum* and *Helminthosporium solani* (Demissie et al., 2020, 2018; Lysøe et al., 2017; Nygren et al., 2018; Piombo et al., 2021) to investigate whether the altered antagonistic ability of Δ*sre1* is due to a change in the expression of antagonism-responsive *C. rosea* genes. In this study, *C. rosea* genes upregulated during interactions with fungal hosts were considered antagonism-related genes. We found 27 differentially expressed antagonism-related genes in the Δ*sre1*, compared to the WT. Of these, 18 genes were downregulated in Δ*sre1* compared to the WT in CZ, including genes coding for polyketide synthases (*pks22*, *pks23*, *pks29*), MFS transporters (*mfs104*, *mfs524*, *mfs533*), proteases, peptidases, chitinases and Cathepsin A (Fig. 7).

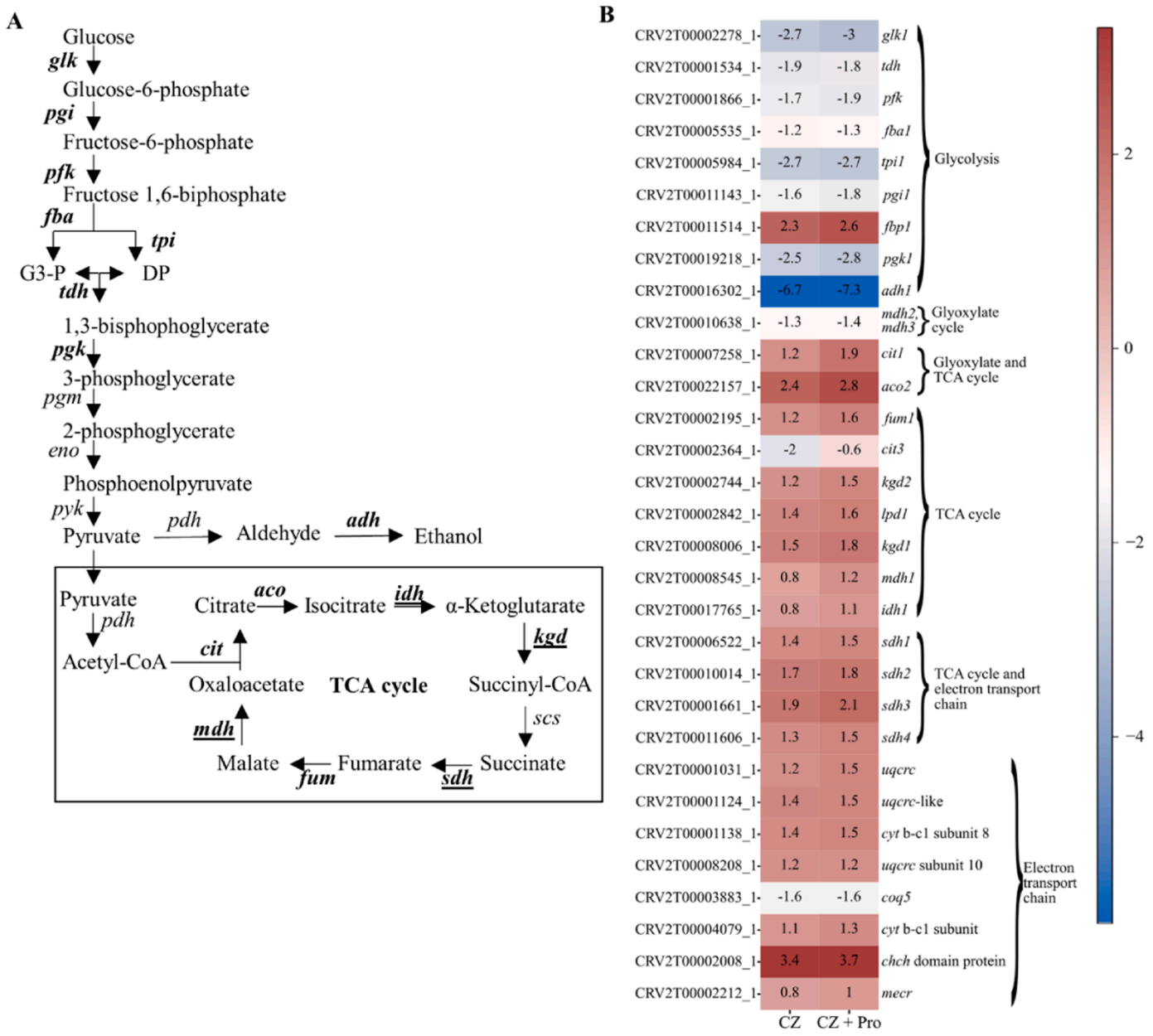

Fig. 6. **A**: Gene involved in glycolysis, glyoxylate cycle, TCA cycle, or electron transport chain differentially expressed in Δ*sre1*. Gene significantly upregulated or in Δ*sre1* compared to the WT are marked with bold letters. A downregulated gene (*erg1*) is marked with bold and underlined letters. **B**: The log2(FC) of the deletion mutant compared to the WT is shown in the heatmap. All differentially expressed genes were determined using DESeq2 (Love et al., 2014) with an adjusted p-value of ≤ 0.05 and log2FC threshold of 1. Red and blue colours represent up-regulated and down-regulated genes, respectively. GLK, Hexokinase;, PGI, Glucose-6-phosphate isomerase; PFK, Phosphofructokinase; FBA, Aldolase; TPI, Triose phosphate isomerase; TDH, Glyceraldehyde-3-phosphate dehydrogenase; PGK, Phosphoglycerate kinase; PGM, Phosphoglycerate mutase; ENO, Enolase: PYK, Pyruvate kinase; G3-P, Glyceraldehyde 3-phosphate; DP, Dihydroxyacetone phosphate; ADH1, Alcohol Dehydrogenase; ACO, Aconitase; IDH, Isocitrate dehydrogenase; KGD, α-ketoglutarate dehydrogenase; SCS, Succinate-Co-A synthetase; SDH, Succinate dehydrogenase; FUM, Fumarase; MDH, malate dehydrogenase; CIT, Citrate synthase; PDH, Pyruvate dehydrogenase; PDC, Pyruvate decarboxylase.

3.11. Gene expression validation by RT-qPCR

RT-qPCR was used to validate RNA-seq data of four transcripts (*pks22*, *pks23*, *pks29* and *sre2*) in *C. rosea*. RNA seq analysis showed downregulation of these genes in the Δ*sre1* strain compared to *C. rosea* WT. In agreement with RNAseq data, RT-qPCR results showed the downregulation of these genes, corroborating the RNAs-seq result (**Supplementary Figure 8).**

4. Discussion

Genes coding for SREBPs are variably distributed among fungal kingdoms (Chung et al., 2019). We hypothesized that the diversity of SREBP gene copy number is related to fungal adaptations to different ecological niches. The similarity in the gene copy number distribution of SREBP in the SRE1 clade1 (the number of paralogs) among fungal species with diverse lifestyles in order Hypocreales indicates a conserved regulatory mechanism of ergosterol biosynthesis across Hypocreales (Ruan et al., 2019). The phylogenetic analysis and protein structure differences between SRE1 and SRE2 indicate a functional diversification of SREBP in *C. rosea*. This is supported by results from Y2H showing the physical interaction between *C. rosea* SRE1, but not SRE2, and SCAP, corroborating the role of the DUF2014 domain in SREBP-SCAP interaction. Taken together, our data showed the presence of the genetic

Table 3
Genes putatively involved in iron homeostasis differentially expressed in Δ*sre1* compared with the wild type.

Gene name	CZ (log2FC)	CZ + Pro (log2FC)	**Annotation**
CRV2T00003050_1	−6.39	−5.25	Aromatic compound dioxygenase
CRV2T00003220_1	−5.09	−5.31	C6 zinc finger domain-containing protein
CRV2T00014973_1	−4.04	−4.03	Aromatic compound dioxygenase
CRV2T00000008_1	−3.26	−0.21	Heme peroxidase
CRV2T00005055_1	−3.02	−3.04	Prolyl 4-hydroxylase
CRV2T00011478_1	−3.01	−3.59	MFS Fir1 class 2.A.1.16.8
CRV2T00004284_1	−2.79	−3.06	Solute carrier family 40
CRV2T00011921_1	−2.69	−3.29	MFS MirB class 2.A.1.16.7
CRV2T00002411_1	−2.24	−4.05	MFS Str1 class 2.A.1.16.6
CRV2T00008584_1	−1.91	−2.33	MFS Fir1 class 2.A.1.16.8
CRV2T00003046_1	−1.85	−2.63	Iron permease FTR1 family protein
CRV2T00016602_1	−1.59	−1.46	Intradiol ring-cleavage dioxygenase
CRV2T00015809_1	−1.50	−2.56	MFS MirB class 2.A.1.16.7
CRV2T00018513_1	−1.33	−3.43	Rieske domain-containing protein
CRV2T00002476_1	−1.02	−1.14	Oxidoreductase containing protein
CRV2T00008059_1	−0.98	−1.24	MFS Fir1 class 2.A.1.16.8
CRV2T00004385_1	−0.87	−1.47	Methylsterol monooxygenase
CRV2T00003460_1	−0.75	−2.01	MFS Fir1 class 2.A.1.16.8
CRV2T00002317_1	−0.34	−1.20	NADPH-P450 reductase-like protein
CRV2T00003715_1	−0.10	−1.76	MFS MirB class 2.A.1.16.7
CRV2T00011438_1	**0.63**	**1.09**	NADPH-P450 reductase-like protein
CRV2T00005718_1	**0.73**	**1.15**	Fumitremorgin C monooxygenase
CRV2T00005223_1	**0.80**	**1.44**	Intradiol ring-cleavage dioxygenase
CRV2T00011977_1	**0.94**	**1.13**	Cysteine dioxygenase
CRV2T00010630_1	**1.06**	**0.92**	Acireductone dioxygenase
CRV2T00010488_1	**1.23**	**1.18**	MFS Fir1 class 2.A.1.16.8
CRV2T00004379_1	**1.30**	**1.67**	Cysteine dioxygenase-like protein
CRV2T00014139_1	**1.52**	**1.99**	Methylsterol monooxygenase
CRV2T00007365_1	**1.64**	**1.72**	FeS biogenesis
CRV2T00015194_1	**1.71**	**1.74**	Cysteine desulfurase, mitochondrial
CRV2T00016086_1	**2.06**	**2.58**	MFS Str1 class 2.A.1.16.6
CRV2T00007357_1	**2.11**	**2.52**	Mitochondrial carrier domain protein
CRV2T00018337_1	**2.15**	**1.93**	Iron-sulfur cluster assembly protein 1
CRV2T00011132_1	**2.40**	**1.60**	MFS Sit1 class 2.A.1.16.1
CRV2T00000798_1	**2.90**	**2.31**	Fatty acid hydroxylase
CRV2T00003296_1	**4.55**	**3.66**	MFS MirB class 2.A.1.16.7
CRV2T00017286_1	**4.83**	**3.95**	MFS Str1 class 2.A.1.16.1

FDR-adjusted p ≤.05 was considered to determine significant differentially expressed genes. The number indicates gene expression level as a log2 fold change (log2FC) in Δ*sre2* strain compared to the WT. Significantly upregulated genes are indicated in bold; significantly downregulated genes are indicated with a minus sign (–). CZ, czapek-dox; CZ+Pro, Czapek-Dox supplemented with prothioconazole.

machinery required for the SREBP signaling pathway in *C. rosea* and highlighted that SRE1 and SRE2 are different phylogenetically and structurally and potentially have evolved for different roles in *C. rosea*.

The SREBP-mediated regulatory mechanisms of cholesterol and ergosterol biosynthesis are primarily conserved between animals and Ascomycetes fungi (Bien and Espenshade, 2010; Osborne and Espenshade, 2009). However, certain fungal species, including *S. cerevisiae* and *C. albicans,* lack mammalian SREBP homologues and have evolved distinct regulatory mechanisms. In *S. cerevisiae,* for instance, the ergosterol biosynthesis pathway is regulated by Upc2, a Gal4-type zinc finger transcription factor (Butler, 2013; Maguire et al., 2014; Ruan et al., 2019). In the current study, heterologous expression of *C. rosea sre1* in Δ*upc2* strain background failed to rescue *S. cerevisiae* from prothioconazole toxicity. This is in line with previous findings suggesting that the SREBP-mediated sterol regulatory mechanism is unrelated to that regulated by Upc2 and demonstrates evolutionary diversity in sterol regulatory mechanisms among fungi (Liu et al., 2015; Osborne and Espenshade, 2009). However, enhanced tolerance of *S. cerevisiae* WT expressing *C. rosea sre1* to prothioconazole highlights the potential role of SRE1 in conferring tolerance to this fungicide in *C. rosea*. This result suggests the functional diversification between SRE1 and SRE2 in *C. rosea*, as *sre2* overexpression did not affect *S. cerevisiae's* tolerance to prothioconazole. This is corroborated by gene deletion results, where no significant differences in the tested phenotypes were observed between the WT and Δ*sre2*, while Δ*sre1* showed several phenotypic effects.

In line with previous findings (Blatzer et al., 2011; Chung et al., 2019; Liu et al., 2015; Osborne and Espenshade, 2009; Ruan et al., 2017; Willger et al., 2008), deletion of *C. rosea sre1* resulted in phenotypic effects, including lower mycelial growth rate on medium supplemented with chemical compounds, targeting cell membrane biosynthesis. This phenotypic effect plausibly results from the impaired cell membrane function in Δ*sre1* strains under stress conditions. This is explained by the altered growth rate of Δ*sre1* strains on medium supplemented with cell wall stressors and deformation of the mycelial structure on medium supplemented with Proline fungicide. The Δ*sre1* strains showed contrasting phenotypic effects towards cell membrane stressors with a higher sensitivity to SDS and tolerance to caffeine. This may be due to variations in their modes of action on fungal cell membranes. SDS acts on the cell wall membrane and activates the stress response, including Cell Wall Integrity (CWI) signaling and inhibits cell growth, while caffeine activates the CWI pathway via phosphorylation of the down-stream protein kinase (Klis et al., 2002; Kuranda et al., 2006; Nunez et al., 2008). Since SREBP is a positive regulator of ergosterol biosynthesis genes, the upregulation of many of these genes in SRE1 deletion strains is intriguing and plausibly suggests an additional mechanism of gene expression regulation in response to prothioconazole in *C. rosea*. Another plausible explanation is that deletion of *sre1* forms a negative transcriptional feedback loop, resulting in the upregulation of ergosterol biosynthesis genes to maintain cellular homeostasis.

Membrane transporters such as ABC and MFS can mediate the efflux of a wide range of drugs and fungicides across the membrane (Coleman and Mylonakis, 2009; Lamping et al., 2010), and upregulation of this class of membrane transporters is one of the nontarget-site mechanisms of drug and fungicides including azole resistance in fungi (Hu and Chen, 2021; Yin et al., 2023). Reduced growth rate, coupled with downregulation of many ABC and MFS transporters in Δ*sre1* strains, underpins the role of this group of proteins in tolerance of Proline and Cantus fungicides in *C. rosea*. Among the downregulated MFS transporters, for example, we identified 11 genes showing similarity with MFS1 previously characterized for its role in fungicide tolerance in the plant pathogenic fungi *B. cinerea*, *Mycosphaerella graminicola*, human pathogenic fungus *Trichophyton rubrum* and the fungal biocontrol agent *Trichoderma harzianum* (Liu et al., 2012; Roohparvar et al., 2007; Samaras et al., 2021; Yamada et al., 2021). Additionally, we identified three downregulated ABC transporter genes (*abcB4* and *abcB18* from group B, multidrug-resistant; *abcC14* from group C, multidrug resistance-associated proteins) in Δ*sre1,* upregulated in culture filtrates containing secreted secondary metabolites from biocontrol bacteria *Pseudomonas chororaphis* and *Serratia rubidaea* S55 (Kamou et al., 2016; Karlsson et al., 2015). Similarly, CYP, a membrane-bound heme protein, catalyzes many reactions involved in drug metabolism, lipids biosynthesis, and iron homeostasis, thereby playing a pivotal role in fungal secondary metabolisms and xenobiotic/drug detoxification (Chen et al., 2014; Manikandan and Nagini, 2018). Downregulation of CYP genes in Δ*sre1* validates its reduced growth rate in presence of Proline and Cantus fungicides. This is in line with previous findings showing upregulation of CYP genes in *T. atroviride* in the presence of pesticide dichlorvos, and

Table 4
Number and class of MFS and ABC transporters differentially expressed in Δ*sre1* compared with the wild type.

MFS class	TCDB Role[#]	Upregulated in CZ	Downregulated in CZ	Upregulated in CZ+Pro	Downregulated in CZ+Pro
2.A.1.1	Sugar Porters (SP)	18	24	13	27
2.A.1.12	Sialate:H+ Symporters (SHS)	0	0	0	1
2.A.1.13	Monocarboxylate Transporters (MCT)	10	7	9	6
2.A.1.14	Anion:Cation Symporters (ACS)	12	15	13	11
2.A.1.16	Siderophore-Iron Transporters (SIT)	5	5	4	5
2.A.1.19	Organic Cation Transporters (OCT)	1	2	2	3
2.A.1.2	Drug:H+ Antiporters−1 (12 Spanner) (DHA1)	28	17	28	15
2.A.1.3	Drug:H+ Antiporters−2 (14 Spanner) (DHA2)	14	12	13	10
2.A.1.48	Vacuolar Basic Amino Acid Transporters (V-BAAT)	2	0	3	0
2.A.1.53	Proteobacterial Intraphagosomal Amino Acid Transporters (Pht)	0	0	1	0
2.A.1.7	Fucose: H+ Symporters (FHS)	0	1	0	3
2.A.1.9	Phosphate: H+ Symporters (PHS)	1	1	1	2
ABC class¤	Description of the class				
FG_ABC_A	Lipid transport and metabolism	0	1	0	1
FG_ABC_B	Multidrug resistance	9	5	6	5
FG_ABC_C	Detoxification of toxic compunds	4	4	4	3
FG_ABC_F	Translation, not transport	2	0	4	0
FG_ABC_G	Pleiotropic drug resistance	9	6	8	4
FG_ABC_ICaf16p	Unknown	2	0	2	0
FG_ABC_Ydr061r	Unknown	1	0	1	0

[#]MFS transporters were classified according to their transporter classification database (TCDB) role (Saier Jr et al., 2021), while ¤ABC transporters were classified according to the classification of Kovalchuk and Driessen (2010). CZ: czapek-dox medium; CZ+Pro: czapek-dox medium supplemented with the prothioconazole.

functional characterization of Ta*Cyp*548–2 by gene deletion demonstrated its involvement in dichlorvos degradation (Hayashi et al., 2002; Nakaune et al., 1998; Omrane et al., 2015; Sun et al., 2022; Whaley et al., 2018; Zhang et al., 2012). Together, these results highlight that the nontarget-site mechanism mediated by membrane transporters and CYP is one of the crucial traits of intrinsic fungicide resistance in *C. rosea*.

Since ergosterol biosynthesis is an oxygen-dependent process, and several oxygen-dependent enzymes are iron-containing, responses to lipid and carbohydrate metabolism, hypoxia and iron homeostasis are often coregulated (Chung et al., 2014; Liu et al., 2015; Osborne and Espenshade, 2009; Willger et al., 2008). Reduced growth of Δ*sre1* in presence of $CoCl_2$ aligns with these previous findings. Downregulation of genes involved in glycolysis and fermentation, showed SRE1 as a positive regulator of glycolysis in *C. rosea*. The upregulation of the TCA cycle in the mutant may be due to a negative feedback regulation mechanism caused by the reduced abundance of glycolysis-generated pyruvate. Additionally, the upregulation of the TCA cycle genes in the *sre1* deletion strain could result from reprogramming the respiratory metabolic pathway for energy production and redox homeostasis. This explanation is supported by the result from GO term analysis where the upregulated genes were significantly enriched in GO terms associated with glycerol, lipids and amino acids metabolic processes. Our results are in line with previous findings in *A. fumigatus*, which showed the role of SREBP in regulating carbohydrate metabolism (Chung et al., 2014). However, previous studies on *S. pombe* and *C. neoformans* showed that SREBPs are transcriptional activators of anaerobic pathway genes and are redundant for genes involved in glycolysis and TCA cycle (Bien and Espenshade, 2010; Chang et al., 2007; Chun et al., 2007; Todd et al., 2006).

In line with the previous studies, this work showed downregulation of many genes associated with siderophore transport and heme biosynthesis in Δ*sre1*, validating the role of SREBP in iron homeostasis in fungi (Blatzer et al., 2011; Chang et al., 2007). For example, we found siderophore transporters mirB, fir1 and sit1, characterized for their role in iron uptake among the downregulated genes. Similarly, iron permease *ftri*, encoding an iron-sulfur protein (Rieske domain protein), which is one of the catalytic subunits of the cytochrome bc_1 complex (Conte and Zara, 2011; Heymann et al., 2002; Park et al., 2006; Raymond-Bouchard et al., 2012; Stearman et al., 1996) was also downregulated. The altered expression of genes associated with oxygen-requiring lipid metabolic processes further validates the role of *C. rosea* SRE1 as a gene expression regulator required for lipid homeostasis.

Antagonism is a complex process that requires host recognition and the production of extracellular enzymes and secondary metabolites to kill fungal hosts (Jensen et al., 2022). We speculate that the altered antagonistic ability of Δ*sre1* is due to its compromised ability to produce these compounds. This is supported by the transcriptome analysis showing the downregulation of mycohost-responsive polyketide synthase (PKS) genes (*pks22*, *pks23*, *pks29*) together with several MFS transporters (*mfs533*, *mfs104*, and *mfs524*) in Δ*sre1*. The *pks22* and *pks29* genes have been previously characterized for their role in antagonistic and biocontrol ability of *C. rosea*. (Fatema et al., 2018). In addition, we detected in Δ*sre1* the downregulation of two chitinase genes, *chic2* and *ech42*, which were previously characterized for their antagonistic ability against *B. cinerea*, *R. solani* and *F. graminearum*, respectively (Mamarabadi et al., 2008; Tzelepis et al., 2015). Since fungal hosts counterattack by producing enzymes, toxic specialized metabolites, and reactive oxygen species, the ability of mycoparasites to tolerate these compounds is vital for successful antagonism (Broberg et al., 2021; Dubey et al., 2014a; Jensen et al., 2021, Piombo et al., 2021). Therefore, it is not difficult to envision that a compromised ability of Δ*sre1* to tolerate xenobiotics, exemplified by the sensitivity to Proline and Cantus fungicides, SDS or caffeine, could affect *C. rosea* ability to tolerate enzymes and toxic metabolites produced by *R. solani* and consequently its antagonistic ability.

The degree of antagonistic interactions between *C. rosea* and its fungal hosts is host-specific (Piombo et al., 2021, 2024). *C. rosea* can identify its fungal host and respond accordingly, and at the same time, the fungal hosts respond differently to *C. rosea* during interactions (Piombo et al., 2021, 2024). The degree of antagonistic ability of Δ*sre1* towards *R. solani*, *B. cinerea*, and *F. graminearum* in dual plate assays shows a certain level of specificity in SRE1 function. This might be due to variations in protection against secreted compounds from the fungal hosts that are specifically induced during the interactions. The enhanced antagonistic ability of *sre1* deletion strains against *B. cinerea* could also be explained by the fact that several ABC and MFS transporters were upregulated in Δ*sre1*, and many genes of this class have been observed to be important in the antagonistic activity of *C. rosea* (Demissie et al.,

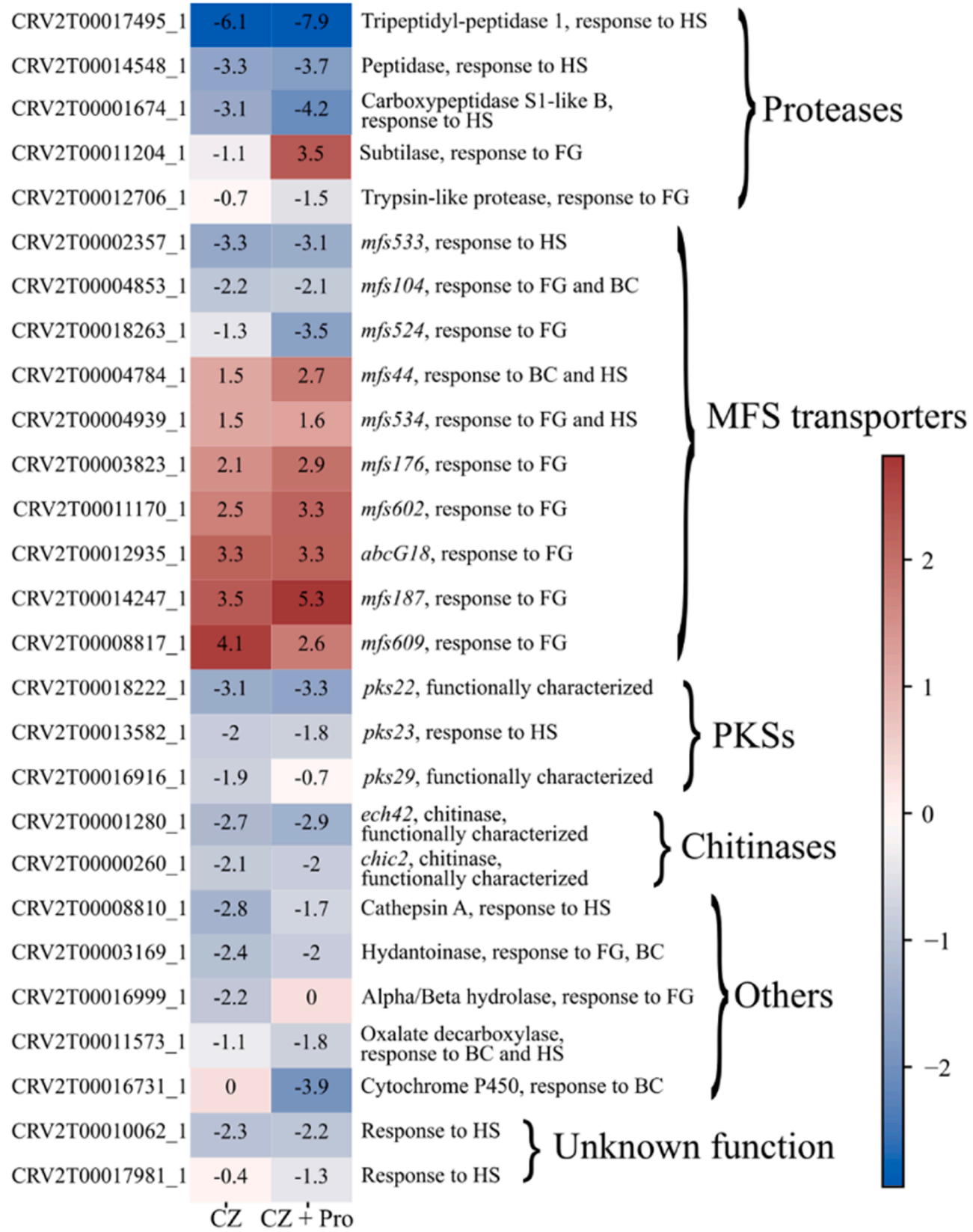

Fig. 7. Genes involved in response to fungal hosts differentially expressed in Δ*sre1*. All differentially expressed genes were determined using DESeq2 (Love et al., 2014) with an adjusted p-value of ≤ 0.05 and log2FC threshold of 1. The log2(FC) of the deletion mutant compared to the WT is shown in the heatmap. All the reported genes were either functionally characterized for their role in mycoparasitism or antagonism (Fatema et al., 2018; Tzelepis et al., 2015), or they were found to be differentially expressed during *C. rosea* interaction with fungal hosts (Demissie et al., 2020; Lysøe et al., 2017; Nygren et al., 2018). Red and blue colours represent up-regulated and down-regulated genes, respectively. HS, *Helminthosporium solanum*; FG, *Fusarium graminearum*; BC, *Botrytis cinerea*.

2020; Nygren et al., 2018). Similar results showing host-specificity during antagonisms were reported previously in studies involving LysM effectors in *C. rosea* (Dubey et al., 2020). Similarly, in another mycoparasite, *Trichoderma virens,* MAP kinase gene deletion strains displayed reduced antagonistic ability against *Sclerotium rolfsii* but not *R. solani* and *Pythium ultimum*.

5. Conclusion

Here, we provided significant insights into the biological and regulatory roles of SREBPs in the mycoparasitic fungus *C. rosea* IK726, focusing on traits relevant to biocontrol, fungicide tolerance and adaptation to hypoxia. We identified two SREBP encoding genes in *C. rosea* IK726 and showed that they are structurally different and have evolved for different roles. We showed that SRE1 plays a role in xenobiotic and hypoxia tolerance and antagonism in *C. rosea*. By comparing *C. rosea* IK726 WT and Δ*sre1* transcriptome, we provided insights into the regulatory role of this gene. The results presented in this study provide valuable insights into the diverse roles of SREBPs in fungal BCAs, offering a deeper understanding of their contributions to biocontrol traits and adaptive responses to environmental stresses, including hypoxia and fungicide tolerance. Exploring the underlying mechanisms of intrinsic fungicide tolerance and biocontrol traits in BCAs is essential to combine the application of fungicides and BCAs, favoring the knowledge-based implementation of IPM strategies in agriculture production systems.

Author statement

MD, GT, AGR, and VR performed the wet lab experiment, generated the data and prepared the samples for sequencing. EP performed the RNA-Seq analysis and visualized the data. MD interpreted and visualized the results. MD, MK and DFJ conceptualized and designed the study. MD wrote the the manuscript. All authors provided feedback on the manuscript. All authors read and approved the final manuscript.

CRediT authorship contribution statement

Mukesh Dubey: Writing – original draft, Visualization, Validation, Supervision, Resources, Project administration, Methodology, Investigation, Formal analysis, Data curation, Conceptualization. **Georgios Tzelepis:** Writing – review & editing, Visualization, Validation, Methodology, Investigation, Formal analysis. **Alma Gustavsson Ruus:** Writing – review & editing, Methodology, Investigation, Data curation. **Edoardo Piombo:** Writing – review & editing, Visualization, Software, Methodology, Formal analysis, Data curation. **Dan Funck Jensen:** Writing – review & editing, Supervision, Resources, Project administration, Funding acquisition. **Magnus Karlsson:** Writing – review & editing, Validation, Supervision, Resources, Project administration, Funding acquisition, Conceptualization. **Vahideh Rafiei:** Writing – review & editing, Methodology, Investigation, Data curation.

Data Availability

This paper's sequencing data is available on European Nucleotide Archive (ENA) under the bioproject PRJEB61889.

Acknowledgement

This work was financially supported by the Department of Forest Mycology and Plant Pathology. MD acknowledge the Swedish Research Council for Environment, Agricultural Sciences and Spatial Planning (FORMAS; grant number 2018–01420, 2021–01461) and The Swedish Research Council, Vetenskapsrådet (VR; grant number 2022–03639). The SNP&SEQ Technology Platform in Uppsala performed sequencing. The facility is part of the National Genomics Infrastructure (NGI) Sweden and Science for Life Laboratory. The SNP&SEQ Platform is also supported by the Swedish Research Council and the Knut and Alice Wallenberg Foundation.

Authors' contributions

MD, GT, AGR, and VR performed the wet lab experiment, generated the data and prepared the samples for sequencing. EP performed the RNA-Seq analysis and visualized the data. MD interpreted and visualized the results. MD, MK and DFJ conceptualized and designed the study. MD wrote the first draft of the manuscript. All authors provided feedback on the manuscript. All authors read and approved the final manuscript.

Appendix A. Supporting information

Supplementary data associated with this article can be found in the online version at doi:10.1016/j.micres.2024.127922.

References

Agatep, R., Kirkpatrick, R.D., Parchaliuk, D.L., Woods, R.A., Gietz, R.D., 1998. Transformation of *Saccharomyces cerevisiae* by the lithium acetate/single-stranded carrier DNA/polyethylene glycol protocol. Tech. Tips Online 3, 133–137. https://doi.org/10.1016/s1366-2120(08)70121-1.

Ahrendt, S.R., Mondo, S.J., Haridas, S., Grigoriev, I.V., 2022. MycoCosm, the JGI's fungal genome portal for comparative genomic and multiomics data analyses. In: Microbial Environmental Genomics (MEG). Springer, pp. 271–291. https://doi.org/10.1007/978-1-0716-2871-3_14.

Altschul, S.F., Gish, W., Miller, W., Myers, E.W., Lipman, D.J., 1990. Basic local alignment search tool. J. Mol. Biol. 215, 403–410. https://doi.org/10.1016/S0022-2836(05)80360-2.

Andrews, S., 2010. FastQC: a quality control tool for high throughput sequence data. URL ⟨https://www.bioinformatics.babraham.ac.uk/projects/fastqc/⟩.

Bien, C.M., Espenshade, P.J., 2010. Sterol regulatory element binding proteins in fungi: hypoxic transcription factors linked to pathogenesis. Eukaryot. Cell 9, 352–359. https://doi.org/10.1128/ec.00358-09.

Blatzer, M., Barker, B.M., Willger, S.D., Beckmann, N., Blosser, S.J., Cornish, E.J., Mazurie, A., Grahl, N., Haas, H., Cramer, R.A., 2011. SREBP coordinates iron and ergosterol homeostasis to mediate triazole drug and hypoxia responses in the human fungal pathogen *Aspergillus fumigatus*. PLoS Genet 7, e1002374. https://doi.org/10.1371/journal.pgen.1002374.

Broberg, M., Dubey, M., Iqbal, M., Gudmundssson, M., Ihrmark, K., Schroers, H.J., Funck Jensen, D., Brandström Durling, M., Karlsson, M., 2021. Comparative genomics highlights the importance of drug efflux transporters during evolution of mycoparasitism in *Clonostachys* subgenus Bionectria (Fungi, Ascomycota, Hypocreales). Evol. Appl. 14, 476. https://doi.org/10.1111/eva.13134.

Broberg, M., Dubey, M., Sun, M.H., Ihrmark, K., Schroers, H.J., Li, S.D., Jensen, D.F., Durling, M.B., Karlsson, M., 2018. Out in the cold: Identification of genomic regions associated with cold tolerance in the biocontrol fungus *Clonostachys rosea* through genome-wide association mapping. Front. Microbiol. 9, 2844. https://doi.org/10.3389/fmicb.2018.02844.

Brückner, A., Polge, C., Lentze, N., Auerbach, D., Schlattner, U., 2009. Yeast two-hybrid, a powerful tool for systems biology. Int. J. Mol. Sci. 10, 2763–2788. https://doi.org/10.3390/ijms10062763.

Bushnell, B., 2019. BBTools: A suite of fast, multithreaded bioinformatics tools designed for analysis of DNA and RNA sequence Data. Jt. Genome Inst. Berkeley, CA, USA, 2018.

Butler, G., 2013. Hypoxia and gene expression in eukaryotic microbes. Annu. Rev. Microbiol. 67, 291–312. https://doi.org/10.1146/annurev-micro-092412-155658.

Chang, Y.C., Bien, C.M., Lee, H., Espenshade, P.J., Kwon-Chung, K.J., 2007. Sre1p, a regulator of oxygen sensing and sterol homeostasis, is required for virulence in *Cryptococcus neoformans*. Mol. Microbiol. 64, 614–629. https://doi.org/10.1111/j.1365-2958.2007.05676.x.

Chaparro, A.P., Carvajal, L.H., Orduz, S., 2011. Fungicide tolerance of *Trichoderma asperelloides* and *T. harzianum* strains. Agric. Sci. 2 301. https://doi.org/10.4236/as.2011.23040.

Chen, W., Lee, M.-K., Jefcoate, C., Kim, S.-C., Chen, F., Yu, J.-H., 2014. Fungal cytochrome p450 monooxygenases: their distribution, structure, functions, family expansion, and evolutionary origin. Genome Biol. Evol. 6, 1620–1634. https://doi.org/10.1093/gbe/evu132.

Chun, C.D., Liu, O.W., Madhani, H.D., 2007. A link between virulence and homeostatic responses to hypoxia during infection by the human fungal pathogen *Cryptococcus neoformans*. PLoS Pathog. 3, e22. https://doi.org/10.1371/journal.ppat.0030022.

Chung, D., Barker, B.M., Carey, C.C., Merriman, B., Werner, E.R., Lechner, B.E., Dhingra, S., Cheng, C., Xu, W., Blosser, S.J., 2014. ChIP-seq and in vivo transcriptome analyses of the *Aspergillus fumigatus* SREBP SrbA reveals a new regulator of the fungal hypoxia response and virulence. PLoS Pathog. 10, e1004487. https://doi.org/10.1371/journal.ppat.1004487.

Chung, H., Kim, S., Kim, K., Hwang, B., Kim, H., Lee, S., Lee, Y., 2019. A novel approach to investigate hypoxic microenvironment during rice colonization by *Magnaporthe*

oryzae. Environ. Microbiol. 21, 1151–1169. https://doi.org/10.1111/1462-2920.14563.
Coleman, J.J., Mylonakis, E., 2009. Efflux in fungi: la piece de resistance. PLoS Pathog. 5, e1000486. https://doi.org/10.1371/journal.ppat.1000486.
Conesa, A., Götz, S., García-Gómez, J.M., Terol, J., Talón, M., Robles, M., 2005. Blast2GO: A universal tool for annotation, visualization and analysis in functional genomics research. Bioinformatics 21, 3674–3676. https://doi.org/10.1093/bioinformatics/bti610.
Conte, L., Zara, V., 2011. The rieske iron-sulfur protein: import and assembly into the cytochrome bc 1 complex of yeast mitochondria. Bioinorg. Chem. Appl. 2011. https://doi.org/10.1155/2011/363941.
Danecek, P., Bonfield, J.K., Liddle, J., Marshall, J., Ohan, V., Pollard, M.O., Whitwham, A., Keane, T., McCarthy, S.A., Davies, R.M., 2021. Twelve years of SAMtools and BCFtools. Gigascience 10, giab008. https://doi.org/10.1093/gigascience/giab008.
Deguine, J.-P., Aubertot, J.-N., Flor, R.J., Lescourret, F., Wyckhuys, K.A.G., Ratnadass, A., 2021. Integrated pest management: good intentions, hard realities. a review. Agron. Sustain. Dev. 41, 38. https://doi.org/10.1007/s13593-021-00689-w.
Demissie, Z.A., Foote, S.J., Tan, Y., Loewen, M.C., 2018. Profiling of the transcriptomic responses of *Clonostachys rosea* upon treatment with *Fusarium graminearum* secretome. Front. Microbiol. 9, 1061. https://doi.org/10.3389/fmicb.2018.01061.
Demissie, Z.A., Witte, T., Robinson, K.A., Sproule, A., Foote, S.J., Johnston, A., Harris, L. J., Overy, D.P., Loewen, M.C., 2020. Transcriptomic and exometabolomic profiling reveals antagonistic and defensive modes of *Clonostachys rosea* action against *Fusarium graminearum*. Mol. Plant-Microbe Interact. 33, 842–858. https://doi.org/10.1094/MPMI-11-19-0310-R.
Dobin, A., Davis, C.A., Schlesinger, F., Drenkow, J., Zaleski, C., Jha, S., Batut, P., Chaisson, M., Gingeras, T.R., 2013. STAR: ultrafast universal RNA-seq aligner. Bioinformatics 29, 15–21. https://doi.org/10.1093/bioinformatics/bts635.
Dubey, M.K., Broberg, A., Jensen, D.F., Karlsson, M., 2013a. Role of the methylcitrate cycle in growth, antagonism and induction of systemic defence responses in the fungal biocontrol agent *Trichoderma atroviride*. Microbiology 159, 2492–2500. https://doi.org/10.1099/mic.0.070466-0.
Dubey, M.K., Broberg, A., Sooriyaarachchi, S., Ubhayasekera, W., Jensen, D.F., Karlsson, M., 2013b. The glyoxylate cycle is involved in pleotropic phenotypes, antagonism and induction of plant defence responses in the fungal biocontrol agent *Trichoderma atroviride*. Fungal Genet. Biol. 58, 33–41. https://doi.org/10.1016/j.fgb.2013.06.008.
Dubey, M.K., Jensen, D.F., Karlsson, M., 2014a. An ATP-binding cassette pleiotropic drug transporter protein is required for xenobiotic tolerance and antagonism in the fungal biocontrol agent *Clonostachys rosea*. Mol. Plant-Microbe Interact. 27, 725–732. https://doi.org/10.1094/MPMI-12-13-0365-R.
Dubey, M.K., Jensen, D.F., Karlsson, M., 2014b. Hydrophobins are required for conidial hydrophobicity and plant root colonization in the fungal biocontrol agent *Clonostachys rosea*. BMC Microbiol 14, 1–14. https://doi.org/10.1186/1471-2180-14-18.
Dubey, M., Jensen, D., Karlsson, M., 2016. The ABC transporter ABCG29 is involved in H2O2 tolerance and biocontrol traits in the fungus *Clonostachys rosea*. Mol. Genet. Genom. 291, 677–686. https://doi.org/10.1007/s00438-015-1139-y.
Dubey, M.K., Ubhayasekera, W., Sandgren, M., Funck Jensen, D., Karlsson, M., 2012. Disruption of the Eng18b ENGase gene in the fungal biocontrol agent *Trichoderma atroviride* affects growth, conidiation and antagonistic ability. PLoS One 7, e36152. https://doi.org/10.1371/journal.pone.0036152.
Dubey, M., Vélëz, H., Broberg, M., Jensen, D.F., Karlsson, M., 2020. LysM proteins regulate fungal development and contribute to hyphal protection and biocontrol traits in *Clonostachys rosea*. Front. Microbiol. 11, 679. https://doi.org/10.3389/fmicb.2020.00679.
Espenshade, P.J., Hughes, A.L., 2007. Regulation of sterol synthesis in eukaryotes. Annu. Rev. Genet. 41, 401–427. https://doi.org/10.1146/annurev.genet.41.110306.130315.
Fatema, U., Broberg, A., Jensen, D.F., Karlsson, M., Dubey, M., 2018. Functional analysis of polyketide synthase genes in the biocontrol fungus *Clonostachys rosea*. Sci. Rep. 8, 1–17. https://doi.org/10.1038/s41598-018-33391-1.
Funck Jensen, D., Dubey, M., Jensen, B., Karlsson, M., 2021. Clonostachys rosea for the control of plant diseases, in: Microbial Bioprotectants for Plant Disease Management. BDS Publishing, pp. 429–471. https://doi.org/10.19103/AS.2021.0093.14.
Güldener, U., Heck, S., Fiedler, T., Beinhauer, J., Hegemann, J.H., 1996. A new efficient gene disruption cassette for repeated use in budding yeast. Nucleic Acids Res 24, 2519–2524. https://doi.org/10.1093/nar/24.13.2519.
Hayashi, K., Schoonbeek, H., De Waard, M.A., 2002. Expression of the ABC transporter BcatrD from *Botrytis cinerea* reduces sensitivity to sterol demethylation inhibitor fungicides. Pestic. Biochem. Physiol. 73, 110–121. https://doi.org/10.1016/S0048-3575(02)00015-9.
Heymann, P., Gerads, M., Schaller, M., Dromer, F., Winkelmann, G., Ernst, J.F., 2002. The siderophore iron transporter of *Candida albicans* (Sit1p/Arn1p) mediates uptake of ferrichrome-type siderophores and is required for epithelial invasion. Infect. Immun. 70, 5246–5255. https://doi.org/10.1128/iai.70.9.5246-5255.2002.
Hu, M., Chen, S., 2021. Non-target site mechanisms of fungicide resistance in crop pathogens: a review. Microorganisms 9, 502. https://doi.org/10.3390/microorganisms9030502.
Jensen, D.F., Dubey, M., Jensen, B., Karlsson, M., 2022. CloJensen, D.F., Dubey, M., Jensen, B., Karlsson, M. 2022. Clonostachys rosea to control plant diseases. Burleigh Dodds Science Publishing, pp 1-44. doi: 10.19103/AS.2021.0093.14nostachys rosea to control plant diseases. Burleigh Dodds Science Publishing 1 (44). https://doi.org/10.19103/AS.2021.0093.14.
Jensen, B., Knudsen, I.M.B., Jensen, D.F., Andersen, B., Nielsen, K.F., Thrane, U., Larsen, J., 2011. Importance of microbial pest control agents and their metabolites in relation to the natural microbiota on strawberry. Pestic. Res.
Jones, P., Binns, D., Chang, H.Y., Fraser, M., Li, W., McAnulla, C., McWilliam, H., Maslen, J., Mitchell, A., Nuka, G., Pesseat, S., Quinn, A.F., Sangrador-Vegas, A., Scheremetjew, M., Yong, S.Y., Lopez, R., Hunter, S., 2014. InterProScan 5: genome-scale protein function classification. Bioinformatics 30, 1236–1240. https://doi.org/10.1093/bioinformatics/btu031.
Kamou, N.N., Dubey, M., Tzelepis, G., Menexes, G., Papadakis, E.N., Karlsson, M., Lagopodi, A.L., Jensen, D.F., 2016. Investigating the compatibility of the biocontrol agent *Clonostachys rosea* IK726 with prodigiosin-producing *Serratia rubidaea* S55 and phenazine-producing *Pseudomonas chlororaphis* ToZa7. Arch. Microbiol. 198, 369–377. https://doi.org/10.1007/s00203-016-1198-4.
Karimi, M., De Meyer, B., Hilson, P., 2005. Modular cloning in plant cells. Trends Plant Sci. 10, 103–105. https://doi.org/10.1016/j.tplants.2005.01.008.
Karlsson, M., Durling, M.B., Choi, J., Kosawang, C., Lackner, G., Tzelepis, G.D., Nygren, K., Dubey, M.K., Kamou, N., Levasseur, A., Zapparata, A., Wang, J., Amby, D.B., Jensen, B., Sarrocco, S., Panteris, E., Lagopodi, A.L., Pöggeler, S., Vannacci, G., Collinge, D.B., Hoffmeister, D., Henrissat, B., Lee, Y.H., Jensen, D.F., 2015. Insights on the evolution of mycoparasitism from the genome of *Clonostachys rosea*. Genome Biol. Evol. 7, 465–480. https://doi.org/10.1093/gbe/evu292.
Katoh, K., Standley, D.M., 2013. MAFFT multiple sequence alignment software version 7: improvements in performance and usability. Mol. Biol. Evol. https://doi.org/10.1093/molbev/mst010.
Klis, F.M., Mol, P., Hellingwerf, K., Brul, S., 2002. Dynamics of cell wall structure in *Saccharomyces cerevisiae*. FEMS Microbiol. Rev. 26, 239–256. https://doi.org/10.1111/j.1574-6976.2002.tb00613.x.
Knudsen, I.M.B., HOCKENHULL, J., JENSEN, D.F., 1995. Biocontrol of seedling diseases of barley and wheat caused by *Fusarium culmorum* and *Bipolaris sorokiniana*: effects of selected fungal antagonists on growth and yield components. Plant Pathol. 44, 467–477. https://doi.org/10.1111/j.1365-3059.1995.tb01669.x.
Kosawang, C., Karlsson, M., Vélëz, H., Rasmussen, P.H., Collinge, D.B., Jensen, B., Jensen, D.F., 2014. Zearalenone detoxification by zearalenone hydrolase is important for the antagonistic ability of *Clonostachys rosea* against mycotoxigenic *Fusarium graminearum*. Fungal Biol. 118, 364–373. https://doi.org/10.1016/j.funbio.2014.01.005.
Kumar, S., Stecher, G., Li, M., Knyaz, C., Tamura, K., 2018. MEGA X: molecular evolutionary genetics analysis across computing platforms. Mol. Biol. Evol. 35, 1547. https://doi.org/10.1093/molbev/msy096.
Kuranda, K., Leberre, V., Sokol, S., Palamarczyk, G., François, J., 2006. Investigating the caffeine effects in the yeast *Saccharomyces cerevisiae* brings new insights into the connection between TOR, PKC and Ras/cAMP signalling pathways. Mol. Microbiol. 61, 1147–1166. https://doi.org/10.1111/j.1365-2958.2006.05300.x.
Lamping, E., Baret, P.V., Holmes, A.R., Monk, B.C., Goffeau, A., Cannon, R.D., 2010. Fungal PDR transporters: phylogeny, topology, motifs and function. Fungal Genet. Biol. 47, 127–142. https://doi.org/10.1016/j.fgb.2009.10.007.
Larkin, M.A., Blackshields, G., Brown, N.P., Chenna, R., McGettigan, P.A., McWilliam, H., Valentin, F., Wallace, I.M., Wilm, A., Lopez, R., 2007. Clustal W and Clustal X version 2.0. bioinformatics 23, 2947–2948. https://doi.org/10.1093/bioinformatics/btm404.
Lee, H., Bien, C.M., Hughes, A.L., Espenshade, P.J., Kyung, J.K., Yun, C.C., 2007. Cobalt chloride, a hypoxia-mimicking agent, targets sterol synthesis in the pathogenic fungus *Cryptococcus neoformans*. Mol. Microbiol. 65, 1018–1033. https://doi.org/10.1111/j.1365-2958.2007.05844.
Letunic, I., Doerks, T., Bork, P., 2009. SMART 6: Recent updates and new developments. Nucleic Acids Res 37, 229–232. https://doi.org/10.1093/nar/gkn808.
Liao, Y., Smyth, G.K., Shi, W., 2014. FeatureCounts: an efficient general purpose program for assigning sequence reads to genomic features. Bioinformatics 30, 923–930. https://doi.org/10.1093/bioinformatics/btt656.
Liu, M., Liu, J., Wang, W.M., 2012. Isolation and functional analysis of Thmfs1, the first major facilitator superfamily transporter from the biocontrol fungus *Trichoderma harzianum*. Biotechnol. Lett. 34, 1857–1862. https://doi.org/10.1007/s10529-012-0972-x.
Liu, J.-Y., Shi, C., Wang, Y., Li, W.-J., Zhao, Y., Xiang, M.-J., 2015. Mechanisms of azole resistance in *Candida albicans* clinical isolates from Shanghai, China. Res. Microbiol. 166, 153–161. https://doi.org/10.1016/j.resmic.2015.02.009.
Livak, K.J., Schmittgen, T.D., 2001. Analysis of relative gene expression data using real-time quantitative PCR and the 2(-Delta Delta C(T)) Method. Methods 25, 402–408. https://doi.org/10.1006/meth.2001.1262.
Love, M.I., Anders, S., Huber, W., 2014. Differential analysis of count data - the DESeq2 package. Genome Biol. 15, 10–1186. https://doi.org/10.1186/s13059-014-0550-8.
Lysøe, E., Dees, M.W., Brurberg, M.B., 2017. A three-way transcriptomic interaction study of a biocontrol agent (*Clonostachys rosea*), a fungal pathogen (*Helminthosporium solani*), and a potato host (*Solanum tuberosum*). Mol. Plant-Microbe Interact. https://doi.org/10.1094/MPMI-03-17-0062-R.
Macedo, P.E.F., Maffia, L.A., Cota, L.V., Lourenço, V., Mizubuti, E.S.G., 2012. Sensitivity of four isolates of *Clonostachys rosea* to pesticides used in the strawberry crop in Brazil. J. Pestic. Sci. 37, 333–337. https://doi.org/10.1584/jpestics.D11-055.
Maguire, S.L., Wang, C., Holland, L.M., Brunel, F., Neuveglise, C., Nicaud, J.-M., Zavrel, M., White, T.C., Wolfe, K.H., Butler, G., 2014. Zinc finger transcription factors displaced SREBP proteins as the major sterol regulators during Saccharomycotina evolution. PLoS Genet 10, e1004076. https://doi.org/10.1371/journal.pgen.1004076.
Mamarabadi, M., Jensen, B., Jensen, D.F., Lübeck, M., 2008. Real-time RT-PCR expression analysis of chitinase and endoglucanase genes in the three-way interaction between the biocontrol strain *Clonostachys rosea* IK726, *Botrytis cinerea*

and strawberry. FEMS Microbiol. Lett. 285, 101–110. https://doi.org/10.1111/j.1574-6968.2008.01228.x.
Manikandan, P., Nagini, S., 2018. Cytochrome P450 structure, function and clinical significance: a review. Curr. Drug Targets 19, 38–54. https://doi.org/10.2174/1389450118666170125144557.
Marchler-Bauer, A., Lu, S., Anderson, J.B., Chitsaz, F., Derbyshire, M.K., DeWeese-Scott, C., Fong, J.H., Geer, L.Y., Geer, R.C., Gonzales, N.R., Gwadz, M., Hurwitz, D.I., Jackson, J.D., Ke, Z., Lanczycki, C.J., Lu, F., Marchler, G.H., Mullokandov, M., Omelchenko, M.V., Robertson, C.L., Song, J.S., Thanki, N., Yamashita, R.A., Zhang, D., Zhang, N., Zheng, C., Bryant, S.H., 2011. CDD: a conserved domain database for the functional annotation of proteins. Nucleic Acids Res 39, 225–229. https://doi.org/10.1093/nar/gkq1189.
Minh, B.Q., Schmidt, H.A., Chernomor, O., Schrempf, D., Woodhams, M.D., Von Haeseler, A., Lanfear, R., 2020. IQ-TREE 2: new models and efficient methods for phylogenetic inference in the genomic era. Mol. Biol. Evol. 37, 1530–1534. https://doi.org/10.1093/molbev/msaa015.
Nakaune, R., Adachi, K., Nawata, O., Tomiyama, M., Akutsu, K., Hibi, T., 1998. A novel ATP-binding cassette transporter involved in multidrug resistance in the phytopathogenic fungus *Penicillium digitatum*. Appl. Environ. Microbiol. 64, 3983–3988. https://doi.org/10.1128/AEM.64.10.3983-3988.1998.
Nunez, L.R., Jesch, S.A., Gaspar, M.L., Almaguer, C., Villa-Garcia, M., Ruiz-Noriega, M., Patton-Vogt, J., Henry, S.A., 2008. Cell wall integrity MAPK pathway is essential for lipid homeostasis. J. Biol. Chem. 283, 34204–34217. https://doi.org/10.1074/jbc.M806391200.
Nygren, K., Dubey, M., Zapparata, A., Iqbal, M., Tzelepis, G.D., Durling, M.B., Jensen, D. F., Karlsson, M., 2018. The mycoparasitic fungus *Clonostachys rosea* responds with common and specific gene expression during interspecific interactions with fungal prey. Evol. Appl. 11, 931–949. https://doi.org/10.1111/eva.12609.
Omrane, S., Sghyer, H., Audéon, C., Lanen, C., Duplaix, C., Walker, A., Fillinger, S., 2015. Fungicide efflux and the MgMFS 1 transporter contribute to the multidrug resistance phenotype in *Zymoseptoria tritici* field isolates. Environ. Microbiol. 17, 2805–2823. https://doi.org/10.1111/1462-2920.12781.
Ons, L., Bylemans, D., Thevissen, K., Cammue, B.P.A., 2020. Combining biocontrol agents with chemical fungicides for integrated plant fungal disease control. Microorganisms 8, 1930. https://doi.org/10.3390/microorganisms8121930.
Osborne, T.F., Espenshade, P.J., 2009. Evolutionary conservation and adaptation in the mechanism that regulates SREBP action: what a long, strange tRIP it's been. Genes Dev. 23, 2578–2591. https://doi.org/10.1101/gad.1854309.
Park, Y.-S., Kim, T.-H., Chang, H.-I., Sung, H.-C., Yun, C.-W., 2006. Cellular iron utilization is regulated by putative siderophore transporter FgSit1 not by free iron transporter in *Fusarium graminearum*. Biochem. Biophys. Res. Commun. 345, 1634–1642. https://doi.org/10.1016/j.bbrc.2006.05.071.
Piombo, E., Vetukuri, R.R., Broberg, A., Kalyandurg, P.B., Kushwaha, S., Funck Jensen, D., Karlsson, M., Dubey, M., 2021. Role of Dicer-dependent RNA interference in regulating mycoparasitic interactions. Microbiol. Spectr. 9, e01099-21. https://doi.org/10.1128/Spectrum.01099-21.
Piombo, E., Vetukuri, R.R., Tzelepis, G., Jensen, D.F., Karlsson, M., Dubey, M., 2024. Small RNAs: A new paradigm in fungal-fungal interactions used for biocontrol. Fungal Biol. Rev. 48, 100356. https://doi.org/10.1016/j.fbr.2024.100356.
Qadri, H., Shah, A.H., Mir, M.A., Qureshi, M.F., Prasad, R., 2022. Quinidine drug resistance transporter knockout *Candida* cells modulate glucose transporter expression and accumulate metabolites leading to enhanced azole drug resistance. Fungal Genet. Biol. 161, 103713. https://doi.org/10.1016/j.fgb.2022.103713.
Raymond-Bouchard, I., Carroll, C.S., Nesbitt, J.R., Henry, K.A., Pinto, L.J., Moinzadeh, M., Scott, J.K., Moore, M.M., 2012. Structural requirements for the activity of the MirB ferrisiderophore transporter of *Aspergillus fumigatus*. Eukaryot. Cell 11, 1333–1344. https://doi.org/10.1128/ec.00159-12.
Roberti, R., Badiali, F., Pisi, A., Veronesi, A., Pancaldi, D., Cesari, A., 2006. Sensitivity of *Clonostachys rosea* and *Trichoderma* spp. as potential biocontrol agents to pesticides. J. Phytopathol. 154, 100–109. https://doi.org/10.1111/j.1439-0434.2006.01069.x.
Roohparvar, R., De Waard, M.A., Kema, G.H.J., Zwiers, L.-H., 2007. MgMfs1, a major facilitator superfamily transporter from the fungal wheat pathogen *Mycosphaerella graminicola*, is a strong protectant against natural toxic compounds and fungicides. Fungal Genet. Biol. 44, 378–388. https://doi.org/10.1016/j.fgb.2006.09.007.
Ruan, R., Li, H., Wang, M., 2019. Functional diversification of sterol regulatory element binding proteins following gene duplication in a fungal species. Fungal Genet. Biol. 131, 103239. https://doi.org/10.1016/j.fgb.2019.103239.
Ruan, R., Wang, M., Liu, X., Sun, X., Chung, K.-R., Li, H., 2017. Functional analysis of two sterol regulatory element binding proteins in *Penicillium digitatum*. PLoS One 12, e0176485. https://doi.org/10.1371/journal.pone.0176485.
Saier Jr, M.H., Reddy, V.S., Moreno-Hagelsieb, G., Hendargo, K.J., Zhang, Y., Iddamsetty, V., Lam, K.J.K., Tian, N., Russum, S., Wang, J., 2021. The transporter classification database (TCDB): 2021 update. Nucleic Acids Res 49, 461–467. https://doi.org/10.1093/nar/gkaa1004.
Samaras, A., Karaoglanidis, G.S., Tzelepis, G., 2021. Insights into the multitrophic interactions between the biocontrol agent *Bacillus subtilis* MBI 600, the pathogen *Botrytis cinerea* and their plant host. Microbiol. Res. 248, 126752. https://doi.org/10.1016/j.micres.2021.126752.
Stearman, R., Yuan, D.S., Yamaguchi-Iwai, Y., Klausner, R.D., Dancis, A., 1996. A permease-oxidase complex involved in high-affinity iron uptake in yeast. Science 271 (80), 1552–1557. https://doi.org/10.1126/science.271.5255.1552.
Stenberg, J.A., Sundh, I., Becher, P.G., Björkman, C., Dubey, M., Egan, P.A., Friberg, H., Gil, J.F., Jensen, D.F., Jonsson, M., 2021. When is it biological control? A framework of definitions, mechanisms, and classifications. J. Pest Sci. 94 (2004), 665–676. https://doi.org/10.1007/s10340-021-01354-7.
Sun, J., Karuppiah, V., Li, Y., Pandian, S., Kumaran, S., Chen, J., 2022. Role of cytochrome P450 genes of *Trichoderma atroviride* T23 on the resistance and degradation of dichlorvos. Chemosphere 290, 133173. https://doi.org/10.1016/j.chemosphere.2021.133173.
Sun, Z.B., Li, S.D., Ren, Q., Xu, J.L., Lu, X., Sun, M.H., 2020. Biology and applications of *Clonostachys rosea*. J. Appl. Microbiol. 129, 486–495. https://doi.org/10.1111/jam.14625.
Thambugala, K.M., Daranagama, D.A., Phillips, A.J.L., Kannangara, S.D., Promputtha, I., 2020. Fungi vs. fungi in biocontrol: an overview of fungal antagonists applied against fungal plant pathogens. Front. Cell. Infect. Microbiol. 10, 604923. https://doi.org/10.3389/fcimb.2020.604923.
Todd, B.L., Stewart, E.V., Burg, J.S., Hughes, A.L., Espenshade, P.J., 2006. Sterol regulatory element binding protein is a principal regulator of anaerobic gene expression in fission yeast. Mol. Cell. Biol. https://doi.org/10.1128/MCB.26.7.2817-2831.2006.
Tsirigos, K.D., Peters, C., Shu, N., Käll, L., Elofsson, A., 2015. The TOPCONS web server for combined membrane protein topology and signal peptide prediction. Nucleic Acids Res 43, W401–W407. https://doi.org/10.1093/nar/gkv485.
Tzelepis, G., Dubey, M., Jensen, D.F., Karlsson, M., 2015. Identifying glycoside hydrolase family 18 genes in the mycoparasitic fungal species *Clonostachys rosea*. Microbiol. (U. Kingd. 161, 1407–1419. https://doi.org/10.1099/mic.0.000096.
Tzelepis, G.D., Lagopodi, A.L., 2011. Interaction between *Clonostachys rosea* IK726 and *Pseudomonas chlororaphis* PCL 1391 against tomato foot and root rot caused by Fusarium oxysporium f. sp. radicis lycopersici. IOBC/wprs Bull. 63, 75–79.
Utermark, J., Karlovsky, P., 2008. Genetic transformation of filamentous fungi by *Agrobacterium tumefaciens*. Protoc. Exch. 119, 631–640. https://doi.org/10.1038/nprot.2008.83.
Wedajo, B., 2015. Compatibility studies of fungicides with combination of *Trichoderma* species under in vitro conditions. Virol. Mycol. 4, 149–153.
Whaley, S.G., Zhang, Q., Caudle, K.E., Rogers, P.D., 2018. Relative contribution of the ABC transporters Cdr1, Pdh1, and Snq2 to azole resistance in *Candida glabrata*. Antimicrob. Agents Chemother. 62, 10–1128. https://doi.org/10.1128/aac.01070-18.
Willger, S.D., Puttikamonkul, S., Kim, K.-H., Burritt, J.B., Grahl, N., Metzler, L.J., Barbuch, R., Bard, M., Lawrence, C.B., Cramer Jr, R.A., 2008. A sterol-regulatory element binding protein is required for cell polarity, hypoxia adaptation, azole drug resistance, and virulence in *Aspergillus fumigatus*. PLoS Pathog. 4, e1000200. https://doi.org/10.1371/journal.ppat.1000200.
Yamada, T., Yaguchi, T., Salamin, K., Guenova, E., Feuermann, M., Monod, M., 2021. Mfs1, a pleiotropic transporter in dermatophytes that plays a key role in their intrinsic resistance to chloramphenicol and fluconazole. J. Fungi 7, 542. https://doi.org/10.3390/jof7070542.
Yin, Y., Miao, J., Shao, W., Liu, X., Zhao, Y., Ma, Z., 2023. Fungicide resistance: progress in understanding mechanism, monitoring, and management. Phytopathology® 113, 707–718. https://doi.org/10.1094/PHYTO-10-22-0370-KD.
Zhang, Y., Zhang, Z., Zhang, X., Zhang, H., Sun, X., Hu, C., Li, S., 2012. CDR4 is the major contributor to azole resistance among four Pdr5p-like ABC transporters in *Neurospora crassa*. Fungal Biol. 116, 848–854. https://doi.org/10.1016/j.funbio.2012.05.002.